geodiversitas

2020 • 42 • 11

Climatic evolution in Western Europe during the Cenozoic: insights from historical collections using leaf physiognomy

Mélanie TANRATTANA, Anaïs BOURA, Frédéric M. B. JACQUES, Loïc VILLIER, François FOURNIER, Arthur ENGUEHARD, Sarah CARDONNET, Guillaume VOLAND, Aude GARCIA, Soraya CHAOUCH & Dario DE FRANCESCHI

MUSÉUM NATIONAL D'HISTOIRE NATURELLE
PUBLICATIONS SCIENTIFIQUES

art. 42 (11) — Published on 14 May 2020
www.geodiversitas.com

Geodiversitas est indexé dans / Geodiversitas *is indexed in:*
– Science Citation Index Expanded (SciSearch®)
– ISI Alerting Services®
– Current Contents® / Physical, Chemical, and Earth Sciences®
– Scopus®

Geodiversitas est distribué en version électronique par / Geodiversitas *is distributed electronically by:*
– BioOne® (http://www.bioone.org)

Les articles ainsi que les nouveautés nomenclaturales publiés dans *Geodiversitas* sont référencés par /
Articles and nomenclatural novelties published in Geodiversitas *are referenced by:*
– ZooBank® (http://zoobank.org)

Geodiversitas est une revue en flux continu publiée par les Publications scientifiques du Muséum, Paris
Geodiversitas *is a fast track journal published by the Museum Science Press, Paris*

Les Publications scientifiques du Muséum publient aussi / *The Museum Science Press also publish:*
Adansonia, ***Zoosystema***, ***Anthropozoologica***, ***European Journal of Taxonomy***, ***Naturae***, ***Cryptogamie*** **sous-sections** ***Algologie***, ***Bryologie***, ***Mycologie***.

Diffusion – Publications scientifiques Muséum national d'Histoire naturelle
CP 41 – 57 rue Cuvier F-75231 Paris cedex 05 (France)
Tél. : 33 (0)1 40 79 48 05 / Fax : 33 (0)1 40 79 38 40
diff.pub@mnhn.fr / http://sciencepress.mnhn.fr

ISSN (imprimé / *print*) : 1280-9659/ ISSN (électronique / *electronic*) : 1638-9395

Climatic evolution in Western Europe during the Cenozoic: insights from historical collections using leaf physiognomy

Mélanie TANRATTANA
Anaïs BOURA
CR2P – UMR 7207 (CNRS, MNHN, Sorbonne Université),
Centre de Recherche sur la Paléobiodiversité et les Paléoenvironnements,
Muséum national d'Histoire naturelle, case postale 38, 57 rue Cuvier, F-75231 Paris cedex 05 (France)
melanie.tanrattana@edu.mnhn.fr (corresponding author)
anais.boura@upmc.fr

Frédéric M. B. JACQUES
14 rue Stoeber, F-67000 Strasbourg (France)
menisperm@gmail.com

Loïc VILLIER
CR2P – UMR 7207 (CNRS, MNHN, Sorbonne Université),
Centre de Recherche sur la Paléobiodiversité et les Paléoenvironnements,
Muséum national d'Histoire naturelle, case postale 38, 57 rue Cuvier, F-75231 Paris cedex 05 (France)
loic.villier@upmc.fr

François FOURNIER
Aix-Marseille Université, CNRS, IRD, Collège de France, CEREGE,
case 67, 3 place Victor Hugo, F-13331 Marseille (France)
fournier@cerege.fr

Arthur ENGUEHARD
Sarah CARDONNET
Guillaume VOLAND
Aude GARCIA
CR2P – UMR 7207 (CNRS, MNHN, Sorbonne Université),
Centre de Recherche sur la Paléobiodiversité et les Paléoenvironnements,
Muséum national d'Histoire naturelle, case postale 38, 57 rue Cuvier, F-75231 Paris cedex 05 (France)

Soraya CHAOUCH
UMR 7245, CNRS-MNHN, Muséum national d'Histoire naturelle,
case postale 38, 57 rue Cuvier, F-75231 Paris cedex 05 (France)
soraya.chaouch@mnhn.fr

Dario De FRANCESCHI
CR2P – UMR 7207 (CNRS, MNHN, Sorbonne Université),
Centre de Recherche sur la Paléobiodiversité et les Paléoenvironnements,
Muséum national d'Histoire naturelle, case postale 38, 57 rue Cuvier, F-75231 Paris cedex 05 (France)
dario.de-franceschi@mnhn.fr

Submitted on 15 February 2019 | accepted on 9 August 2019 | published on 14 May 2020

urn:lsid:zoobank.org:pub:5A2734B5-0414-4740-A576-666DFEA9BE5F

Tanrattana M., Boura A., Jacques F. M. B., Villier L., Fournier F., Enguehard A., Cardonnet S., Voland G., Garcia A., Chaouch S. & De Franceschi D. 2020. — Climatic evolution in Western Europe during the Cenozoic: insights from historical collections using leaf physiognomy. *Geodiversitas* 42 (11): 151-174. https://doi.org/10.5252/geodiversitas2020v42a11. http://geodiversitas.com/42/11

ABSTRACT
A major climatic shift, from a glasshouse world to a colder climate with well-developed ice sheets, occurred during the Cenozoic. Such a transition is recorded in both marine and terrestrial records. The latter is more fragmentary and thus comparatively less well known from a climatic point of view. Leaves are abundant fossil remains, which can be used as terrestrial climatic proxies. In this study, several historical collections from France and Belgium were re-investigated. We applied the Climate Leaf Analysis Multivariate Program in order to document the regional past climate from middle Paleocene to middle Miocene in Western Europe. Our analysis suggest relatively cooler conditions during middle Paleocene, followed by a gradual increase of mean annual temperature and precipitation seasonality during late Paleocene; increased temperature seasonality rather than a global cooling at the Eocene-Oligocene transition; an increase of temperature between early and late Oligocene and warm temperate climate in Western Europe similar to other parts of Europe during middle Miocene. These results are broadly consistent with the global trends observed through the Cenozoic era in the marine record. This study provides new quantitative paleoclimatic estimates for various key periods of the Cenozoic era in Western Europe. The consistency of our results with previous studies based on multiples proxies is in favor of the use of historical collections to reconstruct past climates, as long as sufficient sampling is provided.

KEY WORDS
Fossil leaves, paleoclimate, Cenozoic, CLAMP, terrestrial environment.

RÉSUMÉ
Évolution du climat en Europe occidentale durant le Cénozoïque : apports des collections historiques à travers l'utilisation de la morphologie foliaire.
Durant le Cénozoïque, une transition majeure d'un climat chaud et humide vers un climat plus froid avec des calottes glaciaires bien développées, est observée. Cette transition est documentée dans les registres fossiles marin et continental. En raison de la nature plus fragmentaire de ce dernier, les conditions climatiques continentales sont comparativement moins bien connues. Parmi les restes de plantes conservées dans les sédiments, les feuilles sont particulièrement abondantes et peuvent être utilisées comme proxy climatique terrestre. Dans cette étude, plusieurs collections historiques de France et de Belgique ont été réétudiées. La méthode Climate Leaf Analysis Multivariate Program a été appliquée, afin de documenter le climat régional du Paléocène moyen au Miocène moyen en Europe occidentale. Notre analyse suggère des conditions climatiques relativement fraîches pendant le Paléocène moyen, suivies d'une augmentation graduelle de la MAT et de la saisonnalité des précipitations au cours du Paléocène supérieur, une saisonnalité accrue plutôt qu'une baisse de la MAT à la transition Eocène-Oligocène, une augmentation des températures au cours de l'Oligocène et un climat tempéré chaud semblable au reste de l'Europe durant le Miocène moyen. Dans l'ensemble, ces résultats sont cohérents avec les tendances globales observées au cours du Cénozoïque dans le registre marin. Cette étude fournit de nouvelles estimations quantitatives du climat pour plusieurs périodes-clés du Cénozoïque en Europe occidentale. La cohérence de nos résultats avec les études précédentes, basées sur de multiples approches, est en faveur de l'utilisation des collections historiques pour reconstruire les climats anciens, à condition de disposer d'un large échantillonnage.

MOTS CLÉS
Feuilles fossiles, paléoclimat, Cénozoïque, CLAMP, environnement continental.

INTRODUCTION

During the Cenozoic era, a shift from a warm ice-free world to a colder climate associated with well-developed polar ice sheets occurred. Such a transition was punctuated by various climatic events that have been defined on the basis of geochemical and biological data (Collinson *et al.* 1981; Kennett & Stott 1991; Flower & Kennett 1994; Zachos *et al.* 2008). The first of these events is the rapid increase of sea surface temperature at the Paleocene-Eocene boundary, with a climax known as the Paleocene-Eocene Thermal Maximum (Kennett & Stott 1991; Koch *et al.* 1992; Zachos *et al.* 2003; Gehler *et al.* 2016). The sea surface temperature tend to decrease after the early Eocene extreme warm (Zachos *et al.* 2001, 2008). Notably the 'Terminal Eocene Event' is a major global cooling at the Eocene-Oligocene transition, coeval to the development of the Antarctic Ice Sheet (Collinson *et al.* 1981; Akhmetiev *et al.* 2017). The 'Mid-Miocene Climatic Optimum' is generally considered as the last long term warming event that was not linked to anthropogenic influences (Flower & Kennett 1994; Song *et al.* 2017).

Such a climatic evolution observed throughout Cenozoic has been intensively studied in the marine record. Our record is more fragmentary on the continents, since terrestrial records are generally discontinuous and unevenly distributed. Several proxies are used to reconstruct past terrestrial climates, including geochemistry and Nearest-Leaving relatives (NLR) approach on vertebrates (Barrick *et al.* 1999; Böhme 2003), paleosols (Hamer *et al.* 2007) or macro- and microfloras (Collinson *et al.* 1981; Utescher *et al.* 2011). Among these latter proxies, fossil leaves are commonly used for the reconstruction of terrestrial paleoclimates, using

TABLE 1. — Age, sedimentology, paleoenvironement, number of specimens and GPS coordinates of the fossil sites included in this study.

Locality	Age	Sedimentology	Paleoenvironment	Number of specimens	GPS coordinates
Gelinden	mid to late Selandian	cyclic marls	marine shallow-water	*c.* 850	50°45'25.9"N, 5°15'49.1"E
Menat	Selandian	laminated, bituminous shales	freshwater maar	*c.* 350	46°6'36"N, 2°53'24"E
Sézanne	Thanetian	travertinous limestones	riverine	*c.* 140	48°43'12"N, 3°43'12"E
Célas	Priabonian	laminated to compact limestones	lacustrine to palustrine	*c.* 200	44°07'38.2"N, 4°10'32.1"E
Armissan	Rupelian	marly limestones	lacustrine	*c.* 300	43°11'24"N, 3°5'24"E
Aix-en-Provence	Chattian	gypsiferous marls	lagoonal (coastal plain)/lacustrine	*c.* 600	43°31'48"N, 5°23'24"E
Saint-Bauzile	Tortonian	diatomite	freshwater maar	*c.* 650	44°40'12"N, 4°40'12"E

the relationship with their environment (Bailey & Sinnott 1915, 1916, ; Wolfe 1993, 1995; Mosbrugger & Utescher 1997; Wilf *et al.* 1998). Plant-based proxies has been successfully used in various regions, such as Central Europe (e. g. Mosbrugger *et al.* 2005; Traiser *et al.* 2005; Uhl *et al.* 2006; Uhl & Herrmann 2010), North America (e.g. Wolfe 1980, 1994; Wilf 2000; Wing *et al.* 2005), Asia (e.g. Yang *et al.* 2007; Hao *et al.* 2010; Xing *et al.* 2012; Moiseeva *et al.* 2018; Li *et al.* 2018), South America (e. g. Wing *et al.* 2009; Gregory-Wodzicki 2000), Australia (Greenwood *et al.* 2004) and New Zealand (Kennedy *et al.* 2002).

Two main approaches have been implemented to use fossil leaves as paleoclimatic proxies. On the one hand, the systematic approach (Nearest-Living Relative or NLR approach), with methods such as the Coexistence Approach (CA) (Mosbrugger & Utescher 1997), associates the ecological preferences of the NLR to the fossil taxon. Hence, this approach relies on accurate assignment of the fossil leaves to particular taxa. On the other hand, the physiognomic approach, with methods such as the Leaf Margin Analysis (LMA) or the Climate Leaf Analysis Multivariate Program (CLAMP), is based on the statistic relationship between leaf morphology and climatic variables (Wolfe 1993; Yang *et al.* 2011). The climate predicted by fossil leaves is generally consistent with other proxies (Herman & Spicer 1997; Kennedy *et al.* 2002) and the gradual decrease of temperature during Cenozoic is also traced back in the terrestrial record through fossil leaves (Mosbrugger *et al.* 2005). The evolution of Tertiary climate has been broadly studied in Central and Northern Europe using plant remains (e. g. Collinson *et al.* 1981; Mosbrugger *et al.* 2005; Uhl *et al.* 2006; Bruch *et al.* 2007; Uhl & Herrmann 2010; Utescher *et al.* 2011; Utescher *et al.* 2017; Kunzmann *et al.* 2018). Nevertheless, there are still inconsistencies between the marine and terrestrial records and additional work on terrestrial data is needed to reconcile the two realms (e.g. Naafs *et al.* 2018).

Numerous historical collections of fossil leaves are available in France and Belgium. They represent a valuable source of information of the local past diversity and climate at several key periods of the Cenozoic, such as the late Paleocene warming or the Eocene-Oligocene cooling. An important part of these paleofloras was studied during the 19th and 20th centuries. These emblematic floras can be reinvestigated with quantitative modern approaches in order to better understand the regional climatic evolution of this part of Europe during the Cenozoic era.

Therefore, the aims of this study are: 1) to document the terrestrial paleoclimate in Western Europe from the middle Paleocene to the Miocene, based on the reinvestigation of historical collections using modern quantitative methods; and 2) to compare our results with existing literature based on different approaches or proxies.

MATERIAL AND METHODS

FOSSIL LOCALITIES, SEDIMENTOLOGY AND DATING

Seven fossil sites located in France and Belgium were analyzed (Table 1; Figs 1-8). The paleofloras include numerous leaf impressions and compressions. The studied collections are hosted in the Muséum national d'Histoire naturelle (Paris, France), the Institut royal des Sciences naturelles de Belgique (Brussels, Belgium), the University of Liège (Liège, Belgium) and the Muséum d'Histoire naturelle (Marseille, France). The putative age, sedimentological aspects, number of specimens and number of Operational Taxonomic Units (OTU, Sokal & Sneath 1963) included in each paleoclimatic reconstruction are given in Table 1.

Three localities are Paleocene in age, Menat, Gelinden and Sézanne (Fig. 1A). They are all part of the Atlantic Boreal Province as defined by Kvaček (2010). Gelinden is one of the three Paleocene floral units defined by Kvaček (2010). The Menat deposit is the type-locality of the Menat unit *sensu* Kvaček (2010), which shares affinities with Sézanne paleoflora. Menat and Sézanne vegetations are characterized by the presence of Arctotertiary vegetation elements (Collinson & Hooker 2003). Defined by Engler (1882), the Arctotertiary vegetation concept is characterized by abundant conifers and deciduous trees typical of North America and non-tropical Eurasia. The type-locality of this vegetation is Atanikerdluk in Greenland, where a community of *Metasequoia-Macclintockia-Cercidiphyllum* was described (Koch 1963). Actotertiary floras are considered as deciduous megaphyll vegetation with high ecological tolerances and which uniformly covered the northern high latitudes during upper Paleocene (Mai 1995).

The Gelinden paleoflora (Figs 1A; 2) was first studied by Saporta & Marion (1873, 1878), then by Stockmans (1932, 1960). It was considered dominantly thermophilic (Mai

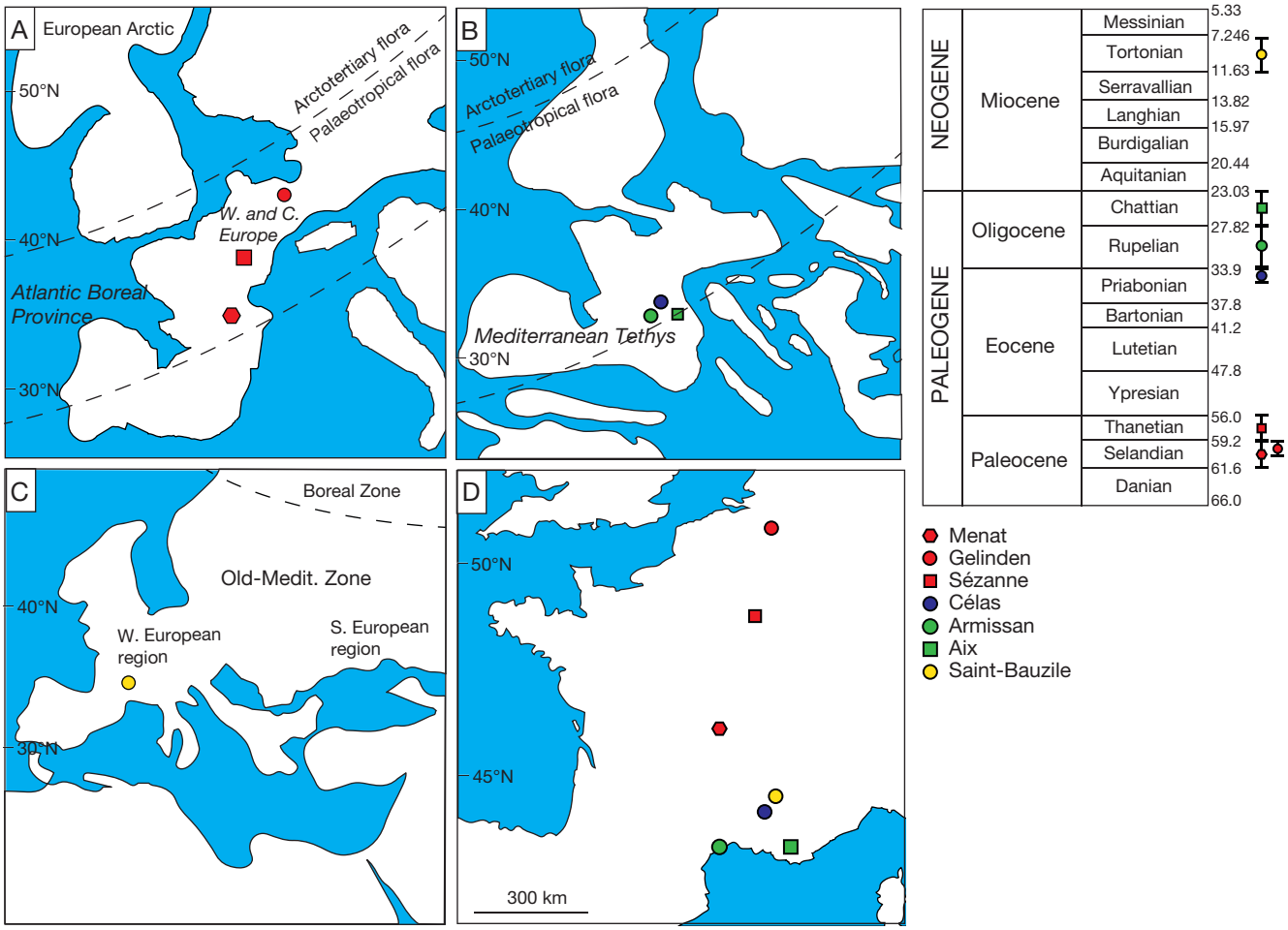

FIG. 1. — Location and chronostratigraphical positions of the deposits: **A**, Paleocene; **B**, Eocene-Oligocene; **C**, Miocene; **D**, present; adapted from Mai (1995), Rögl (1999), Bruch *et al.* (2007) and Kvaček (2010). Information on the provinces and floras are taken from Mai (1995) and Kvaček (2010), in regular and italic fonts respectively.

1995) with abundant evergreen Fagaceae (mostly *Dryophyllum*) and Lauraceae (*Cinnamomum* Schaeff., *Litsea* Lam.). This vegetation was interpreted as evergreen laurophyllous forest or evergreen notophyllous broad-leaved forest (Mai 1995, 1989,1991). The Gelinden paleoflora is preserved in the Gelinden Member, in the upper part of the Heers Formation (Vandenberghe *et al.* 2004; De Bast & Smith 2017). The Gelinden Member is recognized of mid- to late Selandian in age on the basis of the calcareous nannofossil and dinoflagellate associations (Hooyberghs *et al.* 2001).

The Menat deposit is famous for the fine preservation of plant, vertebrate and insect fossil remains (Wedmann *et al.* 2018). The paleoflora of Menat (Figs 1A; 3) has been studied since the 19th century (Brongniart 1828a; Lecoq 1829; Saporta & Marion 1885). The latest revisions of this flora were conducted by Laurent (1912) and Piton (1940). Albeit the flora needs to be revised, Piton (1940) described no less than 90 species within several families such as Salicaceae (*Salix* L.), Fagaceae (*Quercus* L., *Dryophyllum* Debey ex Saporta), Lauraceae (*Laurus* L., *Cinnamomum, Lindera* Thunb.), Fabaceae (*Cassia* L., *Caesalpinia* L.), Ebenaceae (*Diospyros* L.) or Menispermaceae (*Menispermum* L.). The vegetation is considered as a "mixed" forest (Collinson & Hooker 2003), as it includes tropical to subtropical groups along with deciduous elements of the Late Paleocene/Eocene polar deciduous forests (Arctotertiary vegetation), such as *Platanus schimperi* (Heer) Saporta & Marion.

The putative age of the Menat flora have been discussed for many years. Vincent *et al.* (1977) suggested a Thanetian age based on geochemical and palynological analyses. However, the age was revised recently as Selandian (middle Paleocene), based on occurrence of the primate species *Plesiadapis insignis* (Wappler *et al.* 2009), which is supported by ongoing geochemical analyses (F. Quesnel pers. com.).

Saporta (1868) described the paleoflora of Sézanne (Figs 1A; 4), underlining the abundance of megaphylls and its tropical affinities. Later, Langeron (1899) concluded that Sézanne paleoflora had affinities with Asia, Europe and Brazil. In contrary to the two previous authors, Mouton (1970), based on the study of the leaf morphology of Sézanne paleoflora, concluded that the flora had only few tropical affinities. He considered the vegetation as temperate, with the presence of subtropical elements. As for Menat, Collinson & Hooker (2003) considered Sézanne as a "mixed" forest, displaying both

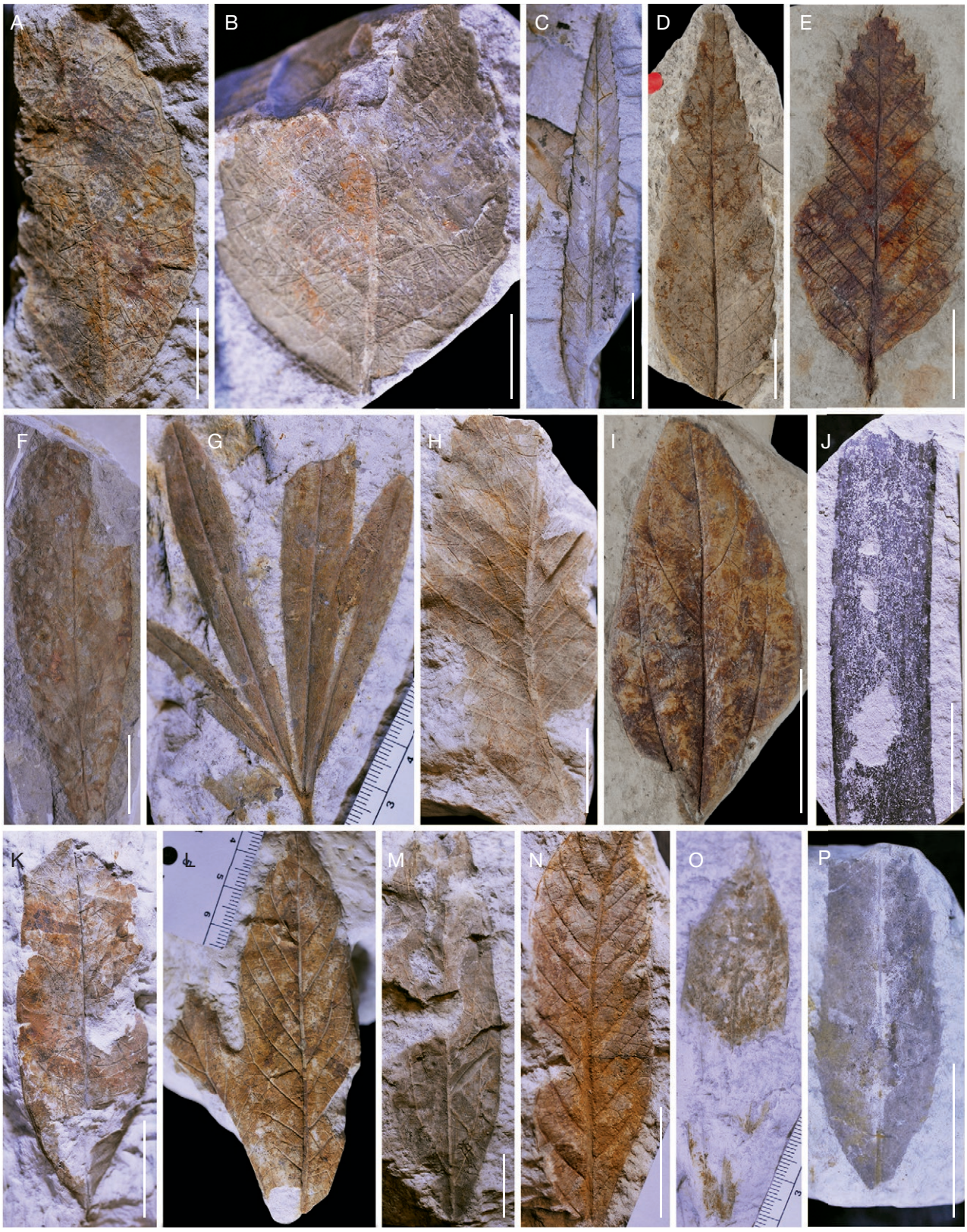

FIG. 2. — Gelinden paleoflora (mid- to late Selandian, Paleocene): **A**, *Quercus odontophylla* Saporta & Marion (IRSNB, 68151); **B**, *Quercus loozi* Saporta & Marion (IRSNB, 68170); **C**, *Dryophyllum curticellense* Saporta & Marion (IRSNB, 68384); **D**, *Dryophyllum dewalquei* Saporta & Marion (MNHN.F.13628); **E**, *Quercus diplodon* Saporta & Marion (MNHN.F.13644); **F**, *Celastrophyllum* sp. (Université de Liège, 2625); **G**, *Dewalquea gelindenensis* Saporta & Marion (IRSNB, 68142); **H**, *Quercus palaeodrys* Saporta & Marion (IRSNB, 68154); **I**, *Cinnamomum ellipsoideum* Saporta & Marion (MNHN.F.13677); **J**, *Posidonia perforata* Saporta & Marion (IRSNB, 68335); **K**, *Aralia transversinervia* Saporta & Marion (IRSNB, 68239); **L**, *Aralia looziana* Saporta & Marion (IRSNB, 68242); **M**, *Litsea elatinervis* Saporta & Marion (IRSNB, 68033); **N**, *Pasianopsis retinervis* Saporta & Marion (IRSNB, 67045); **O**, *Mac-Clintockia heersiennsis* Saporta & Marion (IRSNB, 68034); **P**, *Salix longinqua* Saporta & Marion (IRSNB, 68227). Scale bars: A, B: 1 cm; C-P, 2 cm.

Fig. 3. — Menat paleoflora (Selandian, Paleocene): **A**, *Populus balsamoides* Goeppert (MNHN.F.21144); **B**, *Corylus Mac-Quarrii* (Forbes) Heer (MNHN.F.20734); **C**, *Fraxinus agassiziana* Heer (MNHN.F.12657); **D**, *Salix lamottei* Saporta (MNHN.F.21346); **E**, *Dryophyllum dewalquei* Saporta & Marion (MNHN.F.12665); **F**, *Myrica saportana* Schimper (MNHN.F.20790); **G**, *Dryophyllum curticellense* Saporta & Marion (MNHN.F.21097); **H**, *Quercus elaena* Unger (MNHN.F.21182); **I**, *Acer loetum eocenicum* C. A. Mey (MNHN.F.21157); **J**, *Platanus schimperi* (Heer) Saporta & Marion (MNHN.F.20711); **K**, *Cinnamomum martyi* Fritel (MNHN.F.12646); **L**, *Laurus praecellens* Saporta (MNHN.F.21332); **M**, *Actinodaphne germari* Heer (MNHN.F.21314); **N**, *Lindera stenoloba* (Saporta) Laurent (MNHN.F.21205); **O**, *Quercus lonchitis* Unger (MNHN.F.21300); **P**, *Luheopsis vernieri* Marty (MNHN.F.21165); **Q**, *Ficus tiliaefolia* Heer (MNHN.F.21260); **R**, *Myrica hakeifolia* Saporta (MNHN.F.21323). Scale bars: A-C, E, I-R, 2 cm; D, F, G, H, 1 cm.

FIG. 4. — Sézanne paleoflora (Thanetian, Paleocene): **A**, *Protoficus sezannensis* Saporta (MNHN.F.11873); **B**, *Aralia hederacea* Saporta (MNHN.F.11917); **C**, *Sterculia variabilis* Saporta (MNHN.F.11933); **D**, *Ulmus antiquissima* Saporta (MNHN.F.11870); **E**, *Laurus assimilis* Saporta (MNHN.F.11900); **F**, *Zizyphus raincourtii* Saporta (MNHN.F.11954); **G**, *Daphnogene raincourtii* Saporta (MNHN.F.11906); **H**, *Sassafras primigenium* Saporta (MNHN.F.11902); **I**, *Cissus primaeva* Saporta (MNHN.F.11926); **J**, *Salix stupenda* Saporta (MNHN.F.11880); **K**, *Dryophyllum palaeocastanea* Saporta (MNHN.F.11864); **L**, *Aralia hederacea* Saporta (MNHN.F.11964). Scale bars: A-E, I-L, 2 cm; F-H: 1 cm.

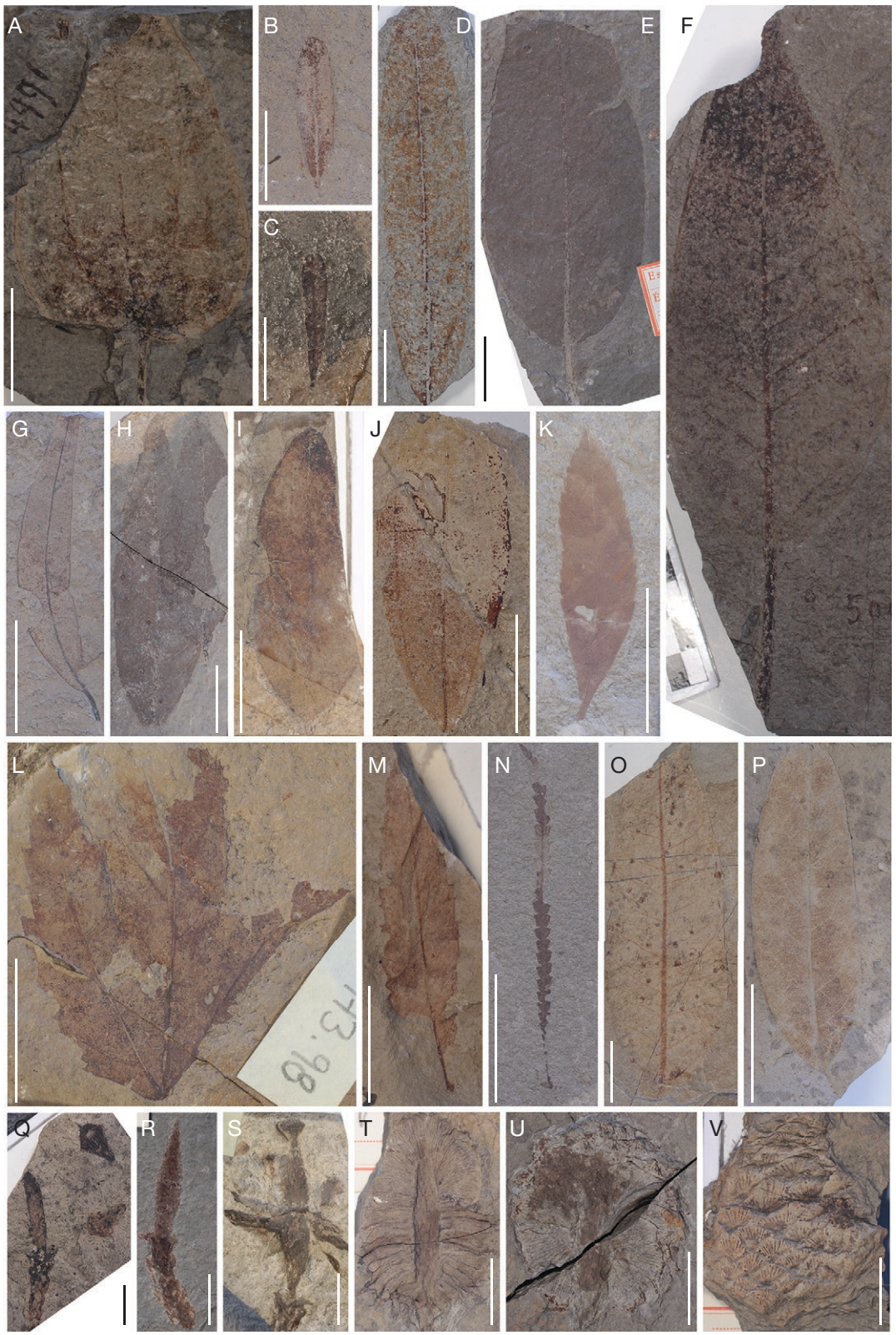

Fig. 5. — Célas paleoflora (Priabonian, Eocene): **A**, *Cocculus intermedius* Laurent (MHN Marseille, 4991); **B**, *Phyllites* sp (MHN Marseille, 4955); **C**, *Parkinsonia recta* Laurent (MHN Marseille, 4966); **D**, *Rhododendron celasensis* Laurent (MHN Marseille, 4988); **E**, *Ficus ovalis* Laurent (MHN Marseille, 4998); **F**, *Ficus marioni* Laurent (MHN Marseille, 5009); **G**, OTU 8 (MHN Marseille, 16733.45); **H**, Indet. (MHN Marseille, 16773.94); **I**, *Andromeda neglecta* Saporta (MHN Marseille, 4987); **J**, *Zizyphus paradisiaca* Heer (MHN Marseille, 4976); **K**, OTU 10 (MHN Marseille, 16773.53); **L**, OTU 19 (MHN Marseille, 16773.98); **M**, ?*Myrica dryandroefolia* Brongniart (MHN Marseille, 16773.39); **N**, OTU 2 (MHN Marseille, 16733.2); **O**, OTU 1 (MHN Marseille, 16773.1.2); **P**, OTU 11 (MHN Marseille, 16773.54). *Doliostrobus* Marion cones at different stages of disintegration. **Q**, MHN Marseille, 16773.20 (Marion 1888: pl. II.16A-B); **R**, MHN Marseille, 16773.18; **S**, MHN Marseille, 16773.16 (Marion 1888: pl. II.15); **T**, MHN Marseille, 16773.14; **U**, MHN Marseille, 16773.17 (Marion 1888: pl. II.13); **V**, MHN Marseille, 16773.12. Scale bars: A, D-P, 2 cm; B, C, Q-V 1 cm.

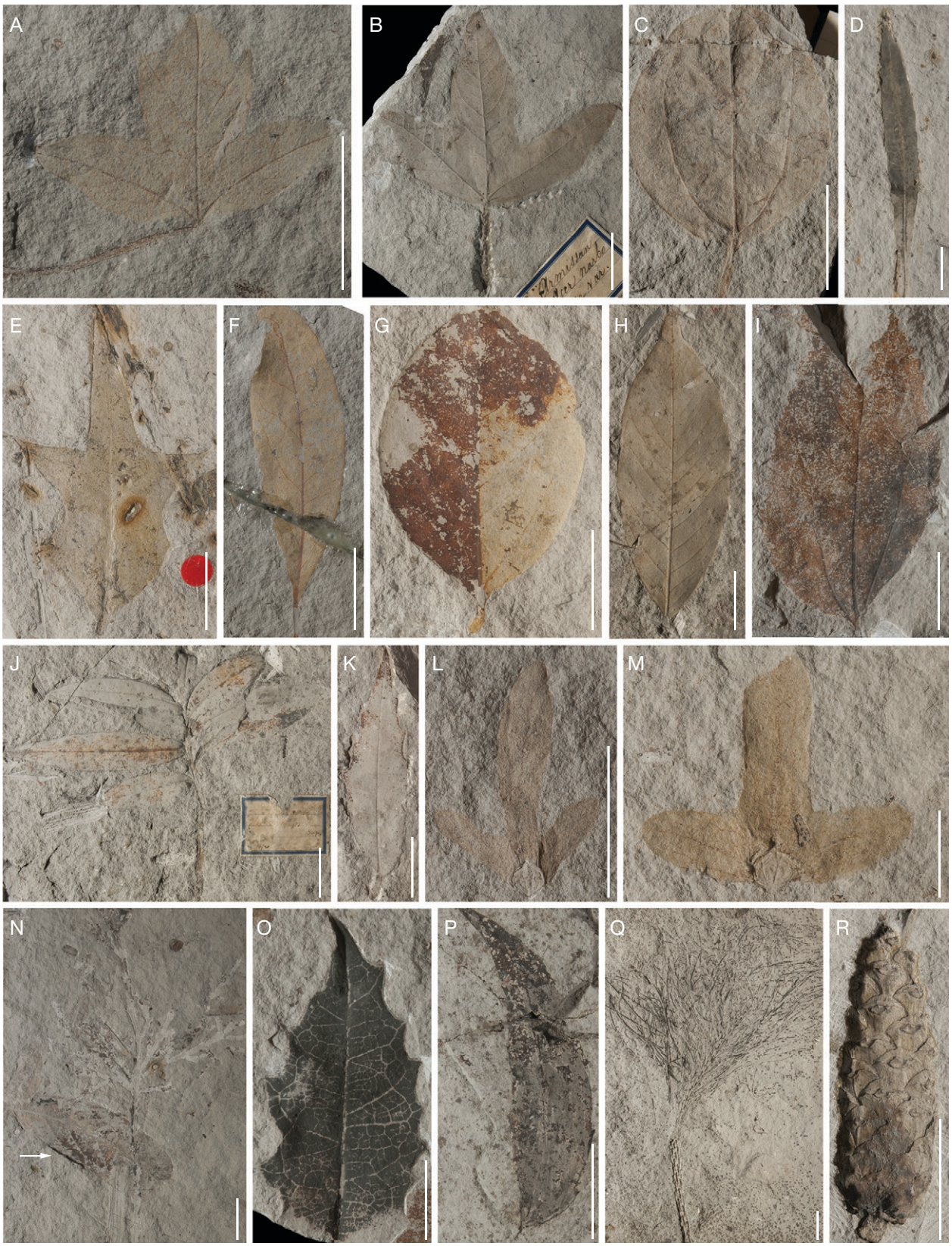

FIG. 6. — Armissan paleoflora (Rupelian, Oligocene): **A**, *Acer pseudocampestre* Unger (MNHN.F.11137); **B**, *Acer narbonense* Saporta (MNHN.F.11139); **C**, *Populus sclerophylla* Saporta (MNHN.F.16043, MNHN.F.16089.B); **D**, *Myrica banksiaefolia* Unger (MNHN.F.12778); **E**, *Quercus armata* Saporta (MNHN.F.12782); **F**, *Laurus resurgens* Saporta (MNHN.F.16033); **G**, *Laurus tournalii* Saporta (MNHN.F.12773); **H**, *Laurus conspicua* Saporta (MNHN.F.12751); **I**, *Celtis primigenia* Saporta (MNHN.F.16099); **J**, *Ilex acuminata* Saporta (MNHN.F.16023); **K**, *Ilex rigida* Saporta (MNHN.F.16048); **L**, *Engelhardtia oxyptera* (MNHN.F.16091); **M**, *Engelhardtia brongniartii* (MNHN.F.12741.2M); **N**, *Myrsine celastroides* Ettingshausen (MNHN.F.11128.2, arrow); **O**, *Ficus dryophylla* Saporta (MNHN.F.16027, 16102); **P**, *Zanthoxylon falcatum* Saporta? (MNHN.F.16038); **Q**, *Pinus divaricata* Saporta (MNHN.F.11169); **R**, *Pinus tenuis* Saporta (MNHN.F.11072). Scale bars: A-L, P-R, 2 cm; M, O, 1 cm.

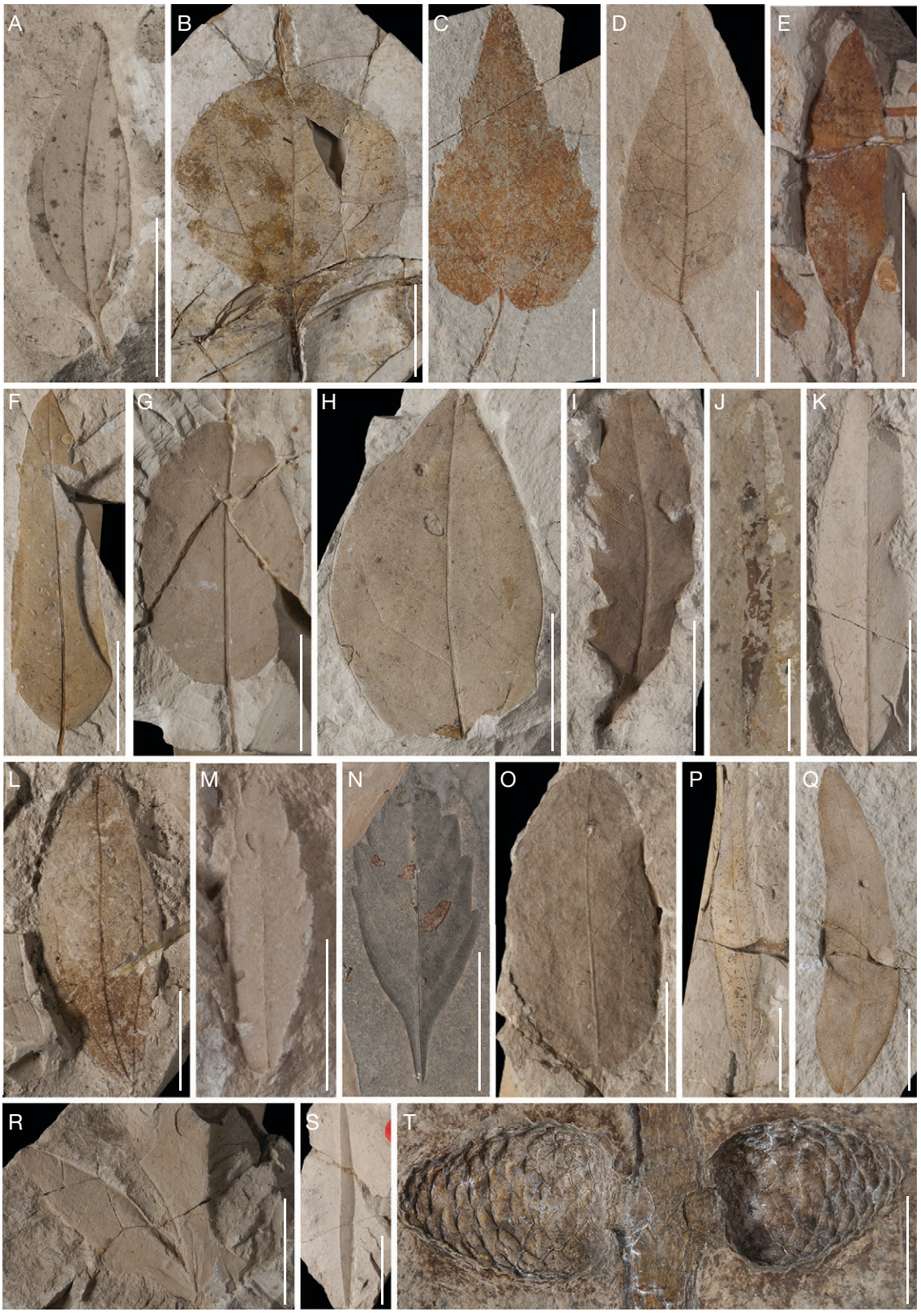

FIG. 7. — Aix-en-Provence paleoflora (Chattian, Oligocene): **A**, *Cinnamomum aquense* Saporta (MNHN.F.16204); **B**, *Cinnamomum polymorphum* (Braun) Heer (MNHN.F.12809); **C**, *Ficus venusta* Saporta (MNHN.F.13969); **D**, *Ficus pulcherrima* Saporta (MNHN.F.13972); **E**, *Myrsine recuperata* Saporta (MNHN.F.14174); **F**, *Diospyros varians* Saporta (MNHN.F.14251); **G**, *Diospyros multinervis* Saporta (MNHN.F.14252); **H**, *Diospyros discreta* Saporta (MNHN.F.14248.1); **I**, *Myrica dryomorpha* Saporta (MNHN.F.28566); **J**, *Myrica angustata* Saporta (MNHN.F.11707); **K**, *Myrsine miramba* Saporta (MNHN.F.14180); **L**, *Oreodaphne detecta* Saporta (MNHN.F.16189); **M**, *Rhus macilenta* (MNHN.F.14153); **N**, *Rhus rhomboidalis* Saporta (MNHN.F.14158); **O**, *Vaccinium obscurum* Saporta (MNHN.F.14645); **P**, *Quercus palaeophellos* Saporta (MNHN.F.13958); **Q**, *Quercus elaena* Unger (MNHN.F.11680); **R**, *Aralia tripartita* Saporta (MNHN.F.14098); **S**, *Podocarpus proxima* Saporta (MNHN.F.16174); **T**, *Pinus coquandii* Saporta (MNHN.F.12818.1M). Scale bars: A-K, N, P-T, 2 cm; L, M, O, 1 cm.

Fig. 8. — Saint-Bauzile paleoflora (Tortonian, Miocene): **A**, *Castanea vesca* Gaertner (MNHN.F.40273); **B**, *Juglans regia* L. (MNHN.F.40289); **C**, *Populus tremula* L. (MNHN.F.40244); **D**, *Quercus cerris* L. (MNHN.F.40225.2); **E**, *Acer decipiens* Braun (MNHN.F.40296); **F**, *Acer campestre* L. (MNHN.F.40318); **G**, *Carpinus* sp. (MNHN.F.40358); **H**, *Quercus* sp. – Ilex group (MNHN.F.40268); **I**, OTU 1 (MNHN.F.40393); **J**, *Crataegus* sp. (MNHN.F.40372); **K**, *Vitis teutonica* Braun (MNHN.F.40585.1); **L**, *Vitis thunbergii* Siebold & Zuccarini (MNHN.F.40228); **M**, *Betula* sp. (MNHN.F.40368); **N**, *Ulmus* sp. (MNHN.F.40366); **O**, *Tilia* sp. (MNHN.F.40323); **P**, OTU 2 (MNHN.F.40394); **Q**, OTU 4 (MNHN.F.40421); **R**, OTU 6 (MNHN.F.40345). Scale bars: A-F, H, I, K-R, 2 cm; G, J, 1 cm.

polar deciduous and warm evergreen elements. The Sézanne Travertine Formation is a freshwater deposit of travertinous limestones (Freytet *et al.* 2001). This formation is assigned to Thanetian in age based on biostratigraphical records (Laurain & Meyer 1986; Gingerich 2000; Freytet *et al.* 2001).

The Célas paleoflora (Figs 1B; 5) is part of the Mediterranean Tethys Province (Kvaček 2010). This flora was described in detail by Laurent (1899). It is characterized by the presence of numerous *Ficus* species and more xerophilous elements such as *Comptonia* L'Hér. ex Aitonor *Zizyphus* Adans. One should mention the presence of *Doliostrobus* (Doliostrobaceae), a conifer represented by numerous leafy shoots, cone scales and cones at different stages of disintegration (Marion 1888; Kvaček 2002a). Part of the collection studied by Marion (1888) was considered missing (Kvaček 2002a, b), but it appears that this material is still hosted in the Marseille Museum (Fig. 5Q-V). Laurent (1899) identified several vegetation belts from the "local" vegetation (with figs and *Doliostrobus* trees surrounding a lake) to the "regional" xerophilous vegetation, characterized by more coriaceous leaves and representative of a seasonal climate, with a dry season. The Célas paleoflora is included in carbonate strata located within a stratigraphic interval ranging from the top of the Lower Carbonate and Evaporite Formation (= LCEF, *sensu* Lettéron *et al.* 2018) to the lower part of the Célas Sandstone Formation. Mammal (Remy 1985, 1994) and charophyte assemblages (Feist-Castel 1971) from upper LCEF and Célas Sandstone formations indicate a middle to late Priabonian age for the Célas paleoflora.

The Armissan paleoflora (Figs 1B; 6) was described by Brongniart (1828b) and Saporta (1865). Mai (1995) defined the Armissan *Florenkomplex*, which is characterized by the presence of Arctotertiary deciduous elements mixed with abundant Lauraceae. The flora includes members of the Taxodiaceae, *Pinus* species (foliage and cones), *Callitris* Vent., *Myrica* L., *Engelhardtia, Ilex* L., *Myrsine* L., *Berberis* L., *Ficus* L., *Zanthoxylon* Walter, *Quercus* L., *Celtis* L., *Ulmus* L., *Acer* L. and *Populus* L. The vegetation is considered as warm temperate (Roiron 1992). The age of the Armissan deposit has been assigned to lower Miocene (Saporta 1865; de Lapparent 1906, 1938; Lavocat 1955). Later, (Schmidt-Kittler 1971) assigned the deposit to the later Oligocene (Rupelian) based on the presence of a particular form of the rodent, *Pseudosciurus* Hensel, similar to the species from the Rupelian of Germany.

The site of Aix-en-Provence (Figs 1B; 7) is famous for its exquisitely preserved fauna (insects and fishes) and flora (Gaudant *et al.* 2017). The latter was studied by Saporta (1863, 1872, 1888a, b), who described 459 species. It includes some conifers (*Pinus* L., *Callitris* Vent. and *Podocarpus* L'Hér. ex Pers.), but also palms, Lauraceae family members, *Ficus* L., *Diospyros* L., *Aralia* L., *Sapindus* L., *Celastrus* L. species and sclerophyllous *Quercus, Dracaena* L., *Myrsine* L., *Myrica* L., *Rhamnus* L., *Zizyphus, Rhus* L. and Fabaceae species (Fig. 7). It was interpreted as sclerophyllous forests developing under a dry, warm climate (Roiron 1992), while the insects of Aix-en-Provence suggest a warm tropical-subtropical climate (Gaudant *et al.* 2017). The flora of Aix-en-Provence was collected in the "Calcaires et marnes à gypse d'Aix" subunit. This subunit was first considered equivalent to the upper part of the gypsiferous sequence of the Paris area (Matheron 1862). Successive authors referred to Aix-en-Provence as Rupelian (Fontannes 1885; Vasseur 1897). The latest studies considered this formation as late Chattian (Oligocene) in age, based on mammal faunas and malacofaunas (Gaudant *et al.* 2017).

The site of Saint-Bauzile is located in the Massif du Coiron, on the eastern border of the Massif Central (Figs 1C; 8). It yielded numerous remains of insects, fishes, amphibians, reptiles and mammals, along with a rich flora (pollen and leaves). The flora of the Massif du Coiron was partly described on material from Rochessauve and Charray by Saporta (1879) and Depape (1912). The first description of the flora discovered in Saint-Bauzile was conducted by Brice (1965). Brice (1965) described 35 species, which display affinities with temperate and Mediterranean Europe, America and Asia. The most abundant remains are attributed to *Quercus, Populus*, *Carpinus* L., *Vitis* L., *Tilia* L., *Castanea* Mill., *Ulmus* L. and *Acer* L. (Brice 1965; Iskandar 1990). The flora shares affinities with the Joursac (Marty 1903) and Rochessauve paleofloras. Based on the analysis of the NLR of this flora, Brice (1965) suggested that the MAT of Saint Bauzile during the Miocene was between 15-20 °C and that precipitations were certainly higher than today. This interpretation is consistent with later work on the microflora, which indicated a warm and moist climate (Iskandar 1990). The Saint-Bauzile flora (Fig. 8) is deposited in a diatomite sequence. The age is supported by radiometric datation of a tephra layer at 7.6-7.2 Ma BP in the lower part of the diatomite sequence (Pastre *et al.* 2004). The mammalian faunal assemblage is consistent with a Tortonian, Late Miocene, age (Métais & Sen 2018).

Methodology

Acknowledging that most of these paleofloras would need careful taxonomic revisions, based on cuticle material (Collinson & Hooker 2003; Kvaček 2010), a taxon-free approach was applied to conduct a first study on the paleoclimatic reconstruction of these historical collections. Future work on cuticle material and venation patterns on these collections might allow us to precise these first results using a taxonomic approach.

Morphological traits of each OTU have been coded for all localities (Table 2), using the spreadsheet available on the website CLAMP Online (Yang *et al.* 2011). Each spreadsheet provides a summary of the leaf morphology in a given locality, by giving the abundance of each morphological trait. This summary was then used to perform a CLAMP analysis on the website CLAMP Online (Yang *et al.* 2011).

CLAMP (Wolfe 1993, 1995; Spicer *et al.* 2009; Yang *et al.* 2011, 2015) is a multivariate analysis, which infers past terrestrial climates based on the extant relationship between leaf morphology and climate. The statistical method underneath CLAMP is the Canonical Correspondence Analysis – CCA (Ter Braak 1986). CCA was introduced to analyze the relationship between species abundance and environmental variables in

TABLE 2. — Morphological trait coding of leaves, completeness scores and number of Operational Taxonomic Units (OTU) for all localities.

Sample	Compl. score	OTU	Lobed	No Teeth	Regular teeth	Close teeth	Round teeth	Acute teeth	Compound teeth	Nanophyll	Lepto 1
Menat	0.83	30	7	37	43	13	8	55	7	0	0
Gelinden	0.62	76	3	45	42	11	13	42	0	0	0
Sézanne	0.75	57	6	60	19	16	2	38	0	0	0
Célas	0.55	70	6	79	1	11	14	8	0	0	2
Armissan	0.91	93	8	60	17	10	5	35	3	1	0
Aix	0.94	206	2	77	14	9	9	14	0	0	4
Saint-Bauzile	0.99	63	18	48	25	10	13	40	5	0	0
	Lepto 2	Micro 1	Micro 2	Micro 3	Meso 1	Meso 2	Meso 3	Em. apex	Round apex	Acute apex	Atten. apex
Menat	0	5	31	32	14	11	6	2	9	64	25
Gelinden	0	0	19	30	28	16	8	6	9	84	6
Sézanne	0	0	4	18	17	20	36	0	13	31	56
Célas	5	23	31	16	3	7	12	9	45	45	3
Armissan	3	13	30	29	18	5	1	3	12	48	40
Aix	9	36	38	8	4	0	0	20	47	31	9
Saint-Bauzile	0	6	30	34	15	8	8	3	19	30	48
	Cordate base	Round base	Acute base	L:W <1:1	L:W 1-2:1	L:W 2-3:1	L:W 3-4:1	L:W >4:1	Obovate	Elliptic	Ovate
Menat	15	11	75	0	26	20	31	22	15	26	59
Gelinden	0	8	94	0	7	19	35	39	9	82	7
Sézanne	3	17	80	3	35	25	26	10	14	59	28
Célas	17	23	60	2	13	43	20	22	14	73	13
Armissan	7	19	74	0	20	33	25	22	12	65	23
Aix	3	28	69	3	22	34	20	21	10	83	8
Saint-Bauzile	15	33	53	17	58	20	4	2	10	75	15

ecology. This purpose is slightly modified in CLAMP, where the abundance of 31 morphological traits measured in several vegetation sites are linked to 11 climatic variables. These include Mean Annual Temperature (MAT), Warm Month Mean Temperature (WMMT), Cold Month Mean Temperature (CMMT), Growing Season Length (GROWSEAS), Growing Season Precipitation (GSP), Mean Monthly Growing Season Precipitation (MMGSP), precipitation during the three consecutive wettest month (3WET), precipitation during the three consecutive driest month (3DRY), annual average relative humidity (RH), annual average specific humidity (SH) and enthalpy (ENTHAL). In practice, the leaf morphologies of tree species from hundreds of sites distributed worldwide form a physiognomic space. The climatic variables are then placed as linear vectors based on the climatic data associated with each locality. The fossil locality is then passively placed among the modern sites and the climatic data is predicted using the score of the fossil site along the linear vector.

To date, four standard calibrations and one exploratory dataset are available: 1) the Physg3brcAZ calibration ("BR" in the following, representing 144 modern vegetation sites mostly from Northern Hemisphere temperate regions, lacking the so-called "alpine nest"); 2) the Physg3arcAZ calibration ("AR" in the following, representing 173 modern vegetation sites mostly from Northern Hemisphere, including the "alpine nest"); 3) the PhysgAsia calibrations ("Asia1" and "Asia2" in the following, suitable for monsoonal climates (Jacques *et al.* 2011; Khan *et al.* 2014)); 4) the Southern Hemisphere calibration (encompassing several areas of the Southern Hemisphere such as Argentina, Bolivia, South Africa, Australia and New Zealand (Kennedy *et al.* 2014); and 5) the PhysGlobal calibration ("Global" in the following, encompassing 378 modern vegetation sites [Yang *et al.* 2015]). The Global calibration is the most complete vision of nowadays world flora. However, the physiognomic space formed by this calibration is very complex (Yang *et al.* 2015), and it is not possible to describe the relationship between leaf physiognomy and climate using linear vectors, as in other classic CLAMP analysis (Yang *et al.* 2015) without increasing the error margin. This calibration is mostly for exploration purposes.

We applied the approach proposed by Teodoridis *et al.* (2011) to choose among the different calibrations. This approach consists in calculating the sum of the differences between the fossil locality scoring and the calibrations scoring for all leaf characters. For instance, if the sum of the differences between the fossil site and the calibration A is higher than the sum of the differences between the fossil site and the calibration B, then one should use the calibration B, i.e. the fossil flora is closer to the calibration B (Teodoridis *et al.* 2011). Calculations for AR and BR showed that all localities were closer to the latter, thus probably not experiencing a very cold winter (freezing temperatures).

In the CLAMP analysis with the Global calibration (Fig. 9A), three localities are close to the monsoonal sites (sites from Asia1 and Asia2 calibrations): Sézanne in particular, Gelinden and Armissan. These three localities are associated with high GSP in both the Global and BR analyses (Fig. 9A, B). According to the approach proposed by Teodoridis *et al.* (2011), the comparison of the differences between Asia1 and Asia2 (Fig. 9C, D) shows that Asia1 calibration is the most suitable calibration for the three potentially monsoonal localities.

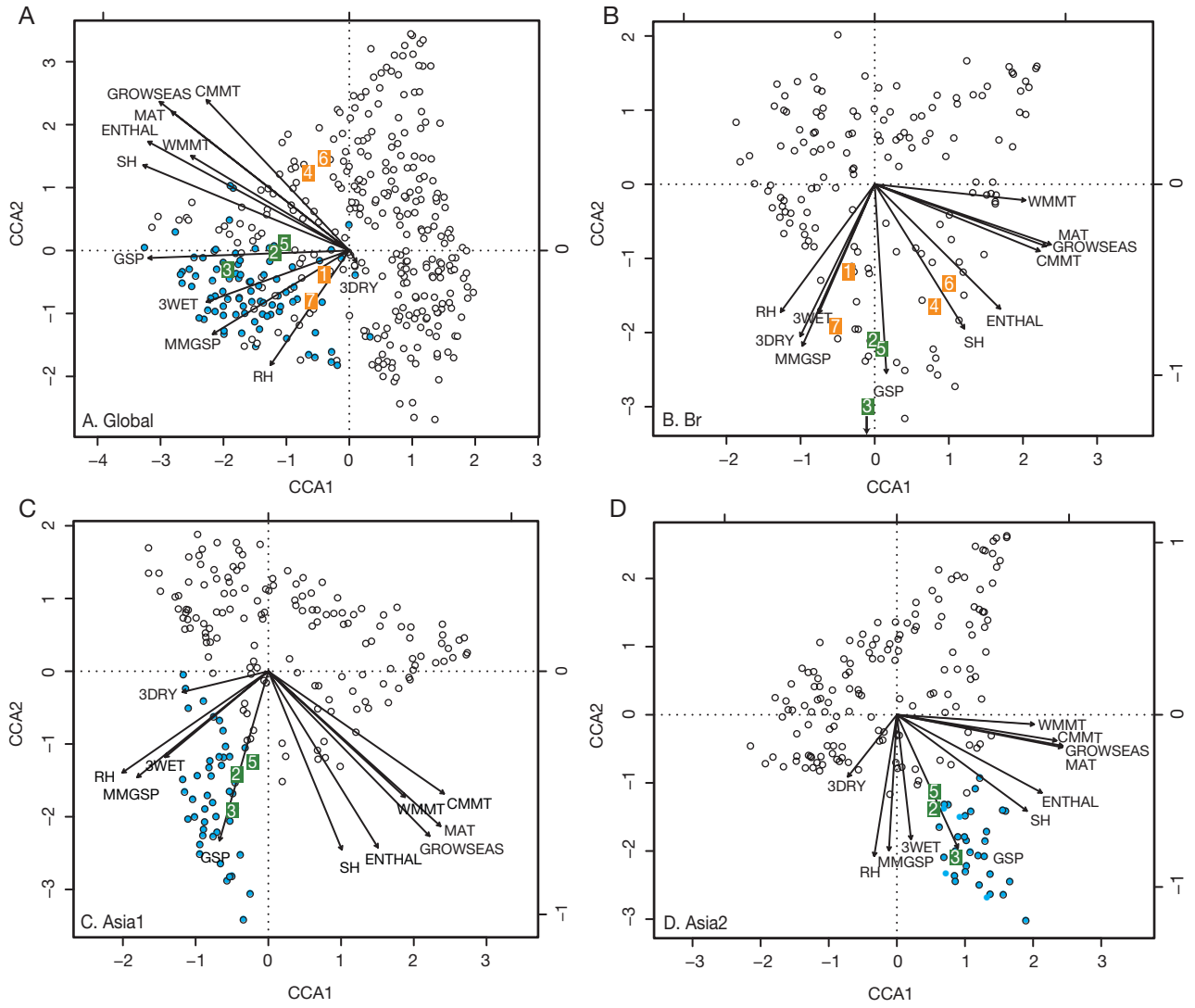

FIG. 9. — Physiognomic spaces showing the location of the fossil sites within the extant sites of **A**, Global calibration, **B**, BR calibration (excluding cold sites), **C**, Asia1 and **D**, Asia2 (both including monsoonal localities: blue filled circles). Numbers: **1**, Menat; **2**, Gelinden; **3**, Sézanne; **4**, Célas; **5**, Armissan; **6**, Aix-en-Provence; **7**, Saint-Bauzile; **green**: localities close to the monsoonal sites.

PALEOCLIMATIC RECONSTRUCTION AND INTERPRETATION

All predicted paleoclimatic variables from the CLAMP analyses are summarized in Table 3. For comparison purposes, GSP was translated into MAP using this proposed calculation: MAP = GSP + (12 – GROWSEA) × (3DRY/3), considering that (1) the growing season includes the most rainy months of the year and (2) MAP includes both GSP and precipitation during the driest months. According to Zhang *et al.* (2016), all the predicted paleoclimates can be interpreted as humid subtropical (Ca-type), with a MAT comprised between 9 and 23°C and a WMMT > 21°C. None of the localities has a CMMT > 18°C, thus the climates can be considered as temperature seasonal.

The highest MAT and CMMT are observed during late Paleocene in Sézanne, late Eocene in Célas and late Oligocene in Aix-en-Provence (Fig. 10). The highest WMMT is observed in Sézanne and the lowest in Célas and Menat (Fig. 10). Highest precipitation are observed in Menat, Célas and Saint-Bauzile (Table 3).

PALEOCENE

The temperatures predicted for Menat and Gelinden (Table 3) suggest that a seasonal warm temperate to subtropical climate, with rather cool winters especially in Menat, was present in Western Europe during Selandian. Our results suggest that the climate of middle Paleocene was colder than reported for late Paleocene and early Eocene in Europe (Fig. 11). At a global scale, the results for Menat and Gelinden are consistent with the MATs predicted in the Amur Region (Russia), Northeast China and North America during early-middle Paleocene (Wilf 2000; Hao *et al.* 2010; Moiseeva *et al.* 2018). This cooler climate, particularly in Menat, is consistent with the short period of cooling climate during middle-late Pale-

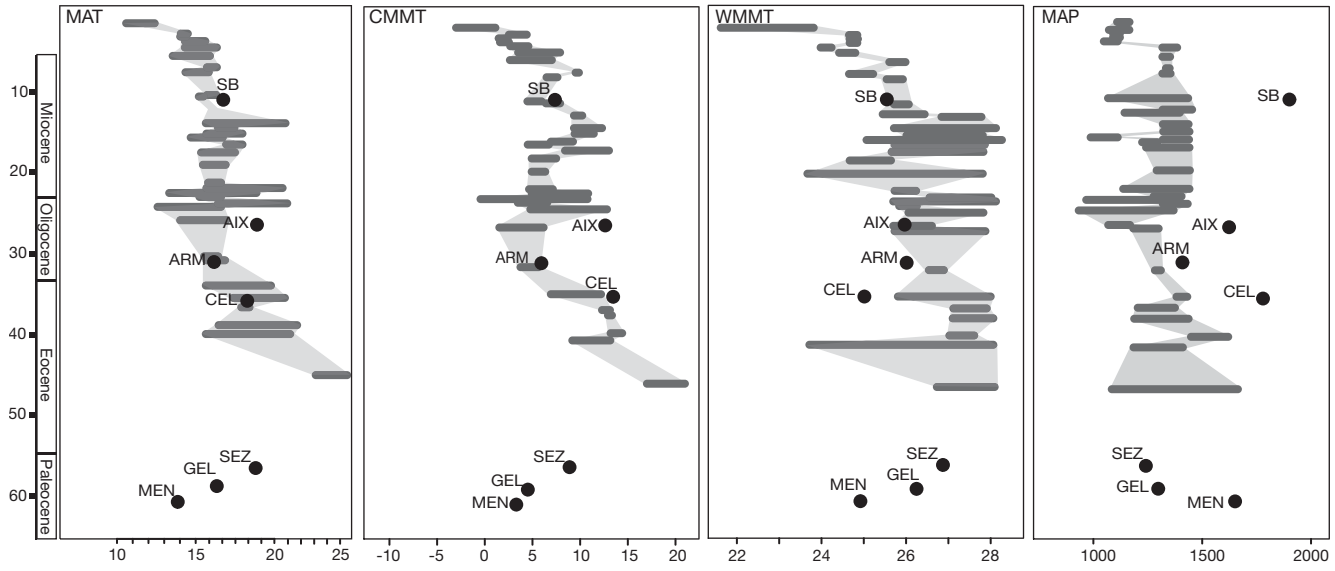

Fig. 10. — Evolution of Mean Annual Temperature (**MAT**), Cold Month Mean Temperature (**CMMT**), Warm Month Mean Temperature (**WMMT**) and Mean Annual Precipitation (**MAP**) in Europe using CLAMP (black dots). For comparison, results obtained with CA are displayed in grey (adapted from Mosbrugger *et al.* 2005). Abbreviations: **MEN**, Menat; **GEL**, Gelinden; **SEZ**, Sézanne; **CEL**, Célas; **ARM**, Armissan; **AIX**, Aix-en-Provence; **SB**, Saint-Bauzile. Numerical values are from Table 3. For Gelinden, Sézanne and Armissan, the results from CLAMP analysis using Asia1 calibration are displayed. For all other localities, the results from CLAMP analysis using BR calibration are displayed.

Table 3. — Paleoclimatic results from CLAMP analyses using BR and Asia1 (**grey background**) calibrations, with associated standard deviation (**SD**). The results used in Figures 9 and 10 are marked with an asterisk.

		MAT °C	WMMT °C	CMMT °C	GROWSEAS months	GSP mm	MAP mm	MMGSP cm	3WET cm	3DRY cm	RH %	SH (g/kg)	ENTHAL 0.1*(kJ/kg)	3WET/3DRY ratio
	SD – Br	2.1	2.5	3.4	1.1	317	–	3.8	22.9	5.9	8.6	1.7	0.8	–
	SD – Asia1	2.5	3.0	4.1	1.3	497	–	5.5	23.9	10.4	7.5	1.8	0.9	–
1	Menat*	13.68	24.89	3.28	7.83	1366	1653.73	19.00	70.91	20.7	74.11	8.04	31.82	3.43
1	Menat	13.03	24.44	2.08	7.88	907.6	1057.98	13.80	54.17	10.95	72.04	7.61	31.64	4.95
2	Gelinden	16.57	26.49	7.04	9.12	1918.9	2152.37	24.06	86.73	24.32	75.40	9.62	32.72	3.57
2	Gelinden *	16.16	26.26	4.93	9.50	1240.6	1327.10	15.35	59.97	10.38	73.40	9.00	32.48	5.78
3	Sezanne	22.09	28.20	14.96	11.77	2647.7	2678.64	30.46	83.48	40.36	84.00	17.45	36.42	2.07
3	Sezanne*	19.29	26.75	8.58	10.99	1224.3	1247.56	15.34	55.40	6.91	81.31	12.92	34.27	8.02
4	Celas*	19.00	25.02	13.50	10.13	1726.9	1837.67	17.02	85.27	17.77	69.47	9.86	33.06	4.80
4	Celas	19.75	26.13	12.59	10.45	1384.4	1464.64	13.39	66.86	15.53	69.87	9.76	33.11	4.31
5	Armissan	16.85	27.17	6.85	9.24	2008.8	2229.23	25.37	89.99	23.96	73.48	9.28	32.61	3.76
5	Armissan*	16.24	25.96	6.10	9.32	1332.5	1453.19	15.11	65.83	13.51	70.74	8.41	32.25	4.87
6	Aix-en-Provence*	19.17	26.03	12.93	10.17	1585.8	1675.17	15.88	80.08	14.65	63.36	8.85	32.67	5.47
6	Aix-en-Provence	20.30	26.13	13.92	10.56	1440.3	1524.49	12.96	69.38	17.54	67.43	9.45	33.03	3.96
7	Saint-Bauzile*	16.33	25.56	7.29	9.13	1636.8	1924.28	21.47	66.48	30.05	83.44	12.34	33.77	2.21
7	Saint-Bauzile	14.21	23.82	4.72	8.25	1050.2	1207.83	14.34	62.52	12.61	77.44	9.28	32.40	4.96

ocene (*c.* 59 Ma), probably associated with the presence of ice sheets in Antarctica (Pancost *et al.* 2013; Hollis *et al.* 2014).

The MATs in Menat and Gelinden are 12-16 °C lower than the temperature obtained in the Fontllonga-3 site (South Central Pyrenees, early Danian) (Fig. 11; Domingo *et al.* 2007). This decrease of temperature is consistent with the regional shift from a warm and humid climate in the early Paleocene (NP1-early NP5), to relatively cooler and drier climate with distinct seasonality in the late Paleocene (NP5-late NP9), observed in Spain and Tunisia (Adatte *et al.* 2000). This cooling is also consistent with the presence, in early Paleocene floras, of deciduous elements from Arctotertiary vegetation, which develops under mesothermic climate (Mai 1989).

For comparison, the climate of the Paleocene is rather well documented in the marine realm. Middle Paleocene (61.6-59.2 Ma) is characterized by climatic variations, with at least two warming events comparable to the PETM, at the Danian-Selandian and Selandian-Thanetian boundaries (Speijer 2003; Dinarès-Turell *et al.* 2007). Cooler conditions than tropical Cretaceous and early Eocene, were certainly prevalent during the Selandian (Buchardt 1977; Wilf 2000; Hollis *et al.* 2012) and our results support this hypothesis.

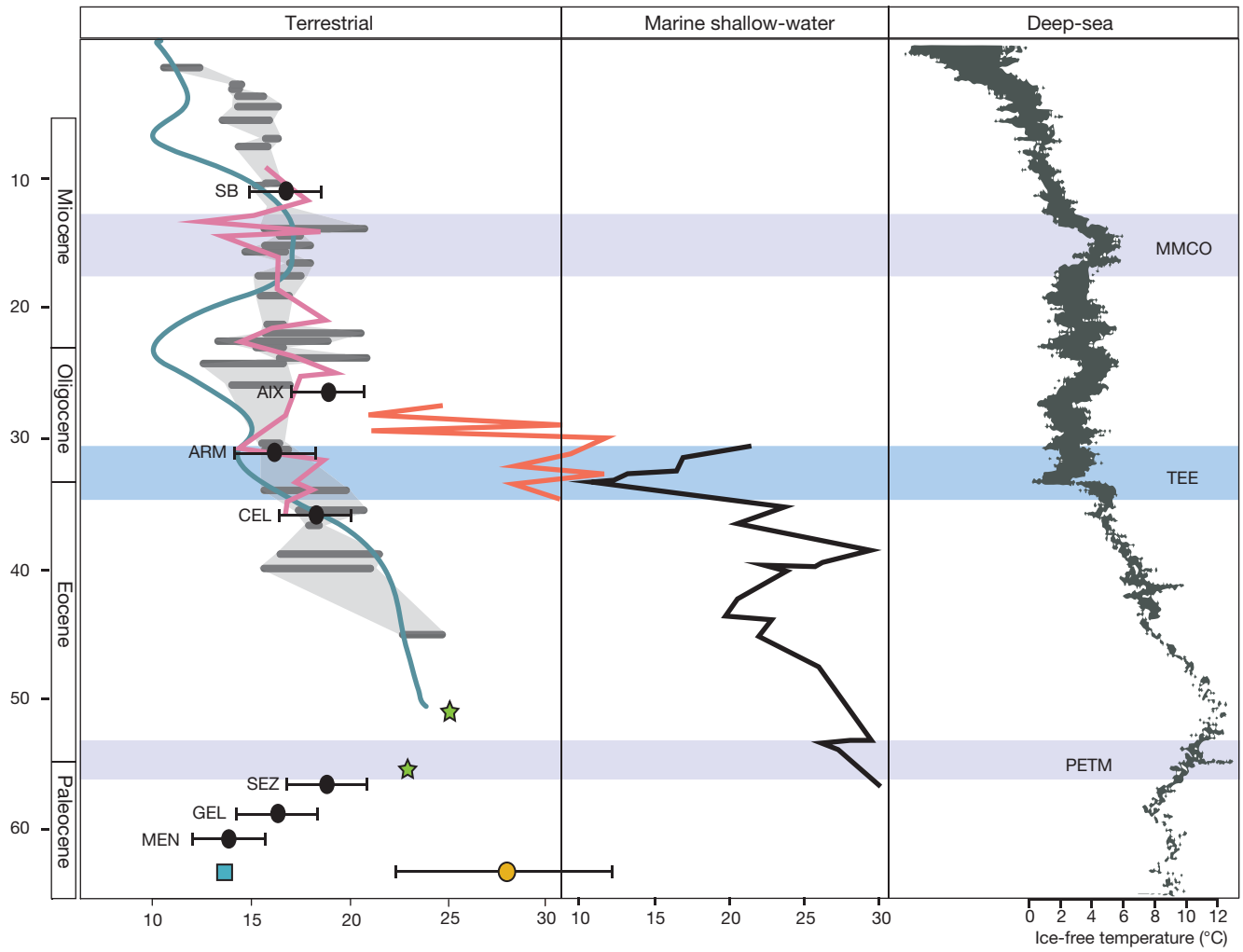

Fig. 11. — Evolution of MAT in Europe in terrestrial, marine shallow-water and deep-sea records. Abbreviations: **MEN**, Menat; **GEL**, Gelinden; **SEZ**, Sézanne; **CEL**, Célas; **ARM**, Armissan; **AIX**, Aix-en-Provence; **SB**, Saint-Bauzile. Symbols: **black circle**, this study, CLAMP on leaves; **light blue solid line**, Bechtel *et al.* (2008), δ13C on coal; **pink solid line**, Héran *et al.* (2010), δ18O on rodents; **orange solid line**, Hren *et al.* (2013), δ47 freshwater gastropods; **grey background**, Mosbrugger *et al.* (2005), CA on leaves; **blue square**, Moiseeva *et al.* (2018), CLAMP on leaves; **yellow circle**, Domingo *et al.* (2007), multi-proxy; **green stars**, Inglis *et al.* (2017), lignites; **black solid line**, Huygue *et al.* (2017), marine mollusks δ18O. Deep-sea record is adapted from Zachos *et al.* (2008). Numerical values are from Table 3. For Gelinden, Sézanne and Armissan, the results from CLAMP analysis using Asia1 calibration are displayed. For all other localities, the results from CLAMP analysis using BR calibration are displayed.

Contrary to previous interpretation based on floral affinities (Saporta 1868; Langeron 1899), the climate predicted for Sézanne is not tropical but rather warm temperate to subtropical as suggested by Mouton (1970). In the leaf morphological data (Table 2), an increase of untoothed leaves proportion is observed from mid Paleocene until Eocene, consistently with Traiser *et al.* (2018) who observed the largest proportion of untoothed margin for the Eocene period in the Morphyll database. The Thanetian stage (59.2-56 Ma) is marked by a gradual increase of the sea surface temperature observed at both global and local scales (Zachos *et al.* 2008; Huyghe *et al.* 2015), until the PETM (*c.* 55 Ma). According to our results, this trend is also observed in continental Western Europe, as an increase of MAT (*c.* 3-6°C), CMMT (*c.* 4-5°C) and WMMT (*c.* 1°C) is recorded from the Selandian to the Thanetian (Table 3; Figs 10, 11). The MAT in Sézanne also contrasts with the very high mean annual sea-surface temperature (MASST) of 30°C, obtained in the Paris basin during latest Paleocene (Fig. 3; Huygue *et al.* 2015). This difference supports the gradual increase of temperature through the Thanetian for this region.

Finally, the MAT reconstructed for all Paleocene localities are lower than the terrestrial temperature estimates (MAT: 23-28°C +/– 4.7°C), based on branched glycerol dialkyl glycerol tetraether (brGDGTs) in early Eocene lignites from Germany and UK (Inglis *et al.* 2017; Naafs *et al.* 2018). Overall, these results suggest that the Paleocene represents a relatively cooler period compared to the Eocene.

We chose to reconstruct the climate of Sézanne and Gelinden using the calibration Asia1, as these localities are nested in the monsoonal localities (Fig. 9A). The differences between the calibrations BR and Asia1 are mainly linked to precipitation parameters, with the latter calibration leading

to lower precipitation values (Jacques *et al.* 2011). In our analysis, results with BR calibration suggest an increase of annual total precipitation between Gelinden and Sézanne (Table 3, BR). There is a slight decrease between the two localities when using Asia1 calibration, although it could be an artifact when taking standard deviation into account (Table 3, Asia1). With Asia1 calibration, precipitation range is more important during Thanetian, with a 3WET/3DRY ratio higher than 6:1 in Sézanne (Table 3, Asia1). The climate of the latter can be characterized as monsoonal (Khan *et al.* 2014), although these values are far from monsoonal climates observed nowadays. This increase of precipitation range during Thanetian is consistent with previous studies focused on the PETM in Europe (Schmitz & Pujalte 2007 and references therein; McInerney & Wing 2011), which suggests higher seasonality of precipitation during this interval rather than higher annual precipitation. Our results suggest that this increase of precipitation seasonality could have started gradually well before the PETM.

Eocene-Oligocene

According to our results, both Célas (middle to late Priabonian, *c.* 36-34 Ma) and Armissan (Rupelian, 33.9-28.1 Ma) floras developed under a warm subtropical climate. Célas is characterized by high precipitation seasonality and mild winter (Table 3). This is in agreement with Laurent's (1912) interpretation of regional xerophilous vegetation, developing under a climate with a dry season. It is also consistent with the subtropical to Mediterranean climate reconstructed in the neighboring Saint-Chaptes basin for the middle and upper Priabonian on the basis of palynological, sedimentological and stable isotope proxies (Lettéron *et al.* 2018). However, it is slightly warmer and moister than the results obtained for the latest Bartonian-early Priabonian Profen-Süd LC flora in Germany (Kunzmann *et al.* 2018).

A decrease of MAT (*c.* 3°C), and particularly CMMT (*c.* 7°C) between Célas and Armissan are observed (Fig. 10). The decrease of MAT between late Eocene and early Oligocene agrees with previous terrestrial climatic estimates (Fig. 11) obtained in Europe from multiple proxies (Fig. 11; Mosbrugger *et al.* 2005; Bechtel *et al.* 2008; Héran *et al.* 2010). It is also consistent with the marine shallow-water and deep-sea record (Fig. 11). However, the MAT decrease is less marked in the terrestrial record (*c.* 3°C), compared to the shallow-marine data where a difference of 12°C before and after Eocene-Oligocene boundary (Huygue *et al.* 2015) and to the temperatures obtained from δ47 on freshwater gastropods (Hren *et al.* 2013).

The Eocene-Oligocene transition (EOT) is marked in the marine record by a positive shift of δ18O, generally interpreted as a general cooling and the establishment of ice sheets in Antarctica (Kennett & Shackleton 1976; Zachos *et al.* 1996; Liu *et al.* 2009). EOT global cooling has been suggested based on both marine and terrestrial proxies (e. g. Mosbrugger *et al.* 2005; Hren *et al.* 2013; Fan *et al.* 2018). Nevertheless, there are some inconsistencies between proxies as some studies rather document a change in temperature seasonality (notably a decrease of winter temperatures) or no global cooling at all (Ivany *et al.* 2000; Grimes *et al.* 2005; Pound & Salzmann 2017). The decrease of CMMT observed in our analysis supports the hypothesis of colder winters (i.e., high seasonal temperature variations) during and after EOT, rather than a global cooling (Mosbrugger *et al.* 2005; Ivany *et al.* 2000). It also suggests an increased temperature seasonal variation in the early Oligocene. Additionally, the climate is globally drier in Armissan, but there is no significant change in precipitation seasonality (Table 3).

After EOT, the MATs reconstructed for Armissan and Aix-en-Provence (Chattian, 28.1-23.03 Ma) are consistent with the temperatures reconstructed for Europe during Oligocene using the Coexistence Approach on micro- and megafloras from Eurasia (Pross *et al.* 2001; Li *et al.* 2018). Our analysis suggests a warm and moist climate in Aix-en-Provence (Table 3), in contrast with previous interpretation based on taxonomic identifications of sclerophyllous vegetation, developing under a dry and warm climate (Roiron 1992). However, it is in agreement with the latest paleoclimatic interpretation based on the insects and fishes of Aix-en-Provence, which suggest a warm tropical to subtropical climate (Gaudant *et al.* 2017). Additionally, an increase of MAP and precipitation seasonality was observed from early to late Oligocene (Table 3; Fig. 10). One explanation to this difference is that Aix-en-Provence paleoflora may be a mixture of several vegetation belts. Notably, six groups were described based on the palynological record: montane vegetation mainly composed of conifers, montane mesophilous forest, low land thermophilous forest, Mediterranean vegetation, littoral vegetation and hygrophilous vegetation (Nury 1990). In this context, Aix-en-Provence could be representative on the lowland thermophilous and Mediterranean vegetations. The presence of elements from the lowland thermophilous forests could bias the results towards a moister climate and to the observed MAP increase. A better knowledge of the taphonomic context of leaves deposition would allow testing this hypothesis. Another possibility is that Aix-en-Provence paleoflora was experiencing high precipitation seasonality and that CLAMP is biased towards the rainy season.

A slight increase in temperatures is observed from early to late Oligocene (*c.* 3°C), leading to a warmer, more equable climate during the Chattian (Table 3; Fig. 10). The increase of temperature from early to late Oligocene was observed in terrestrial central Eurasia, eastern Asia (Li *et al.* 2018), Central Europe (Fig. 11; Héran *et al.* 2010; Kürschner & Kvaček 2009), but also in the marine record (Flower & Chisholm 2006).

Miocene

The climate of Saint-Bauzile (Tortonian, 11.62-7.25 Ma) is interpreted as humid warm temperate to subtropical, consistently with previous interpretation (Brice 1965)

and as previously observed in Central Europe and Spain (Bruch *et al.* 2007). The predicted MAT, CMMT, WMMT and MAP are very close to the results reported for Central Europe and eastern Mediterranean region (Bruch *et al.* 2007, 2011). Our results are also consistent with recent work on the Late Miocene Pannonian Basin (Utescher *et al.* 2017). The MAT of Saint-Bauzile is consistent with climatic estimates obtained from δ13C from coal and δ18O on rodents (Fig. 11). The climate is however more humid than the results obtained by a multiple proxies analysis in the Vallée du Rhone, which suggests a drier environment especially based on fossil mammals (Demarcq *et al.* 1983). Our analysis supports a weak latitudinal climatic gradient in Europe during Middle Miocene as suggested by Bruch *et al.* (2007).

DISCUSSION

The MAT results presented in this study are broadly consistent with the trends observed in the global marine deep-sea record, notably the late Paleocene warming, the EOT cooling and the late Oligocene warming (Fig. 11). As previously observed in terrestrial record (Mosbrugger *et al.* 2005), these trends are more marked in the CMMT than in WMMT (Table 3; Fig. 10). In particular, the decrease of MAT during EOT observed in marine shallow-water environment (Fig. 11) is mirrored in the terrestrial record by a decrease of CMMT, while the WMMT stays relatively stable.

Our results are also globally consistent with previous literature on European paleoclimates obtained from fossil plants but also other terrestrial proxies (Figs 10; 11). This suggests that the CLAMP approach is an appropriate method for reconstructing regional terrestrial paleoclimates based on historical collections, if sufficient sampling is available.

However, there are still some differences between CLAMP and CA (Fig. 10). CA temperatures are generally more homogeneous through time (Uhl *et al.* 2003), yet our results for MAT, CMMT and WMMT fit well with the results predicted by the CA (Fig. 10). The differences are more striking for MAP (Fig. 10), as CLAMP predicted systematically higher precipitation than CA. These discrepancies could be due to regional differences or to a taphonomic bias linked to the vicinity of water (lake, river) (Table 1), which leads to wetter climate predicted by CLAMP. Indeed, CLAMP takes into account intra-specific variability, including the influence of local water availability on leaf size (Peppe *et al.* 2018). Additionally, CLAMP is known for predicting "wetter" climates, as compared to the observed climate (Spicer *et al.* 2011). Nevertheless, the CA results stay within the uncertainty range of CLAMP (Table 3).

Another matter of concern is Sézanne receiving less precipitation than Aix-en-Provence, which might be surprising. Indeed, large mesophylls are most abundant in Sézanne, while microphylls are most abundant in Aix-en-Provence (Table 2). This is mostly due to the different calibrations used to reconstruct the climates of Sézanne (Asia1) and Aix-en-Provence (BR). As stated above, the differences between the BR and Asia1 calibrations are mainly linked to precipitation parameters, with the latter calibration leading to lower precipitation values (Jacques *et al.* 2011). Moreover, this difference stays within the range of the standard deviation (Table 3).

Finally, the studied material comes from historical collections, some of which are disconnected from up-to-date sedimentary settings. It might be an issue as the paleofloras might sample plant species from different paleoenvironments. For instance, a mixture of vegetation in Aix-en-Provence might lead to unexpectedly high precipitation. Despite the fact that CLAMP is supposed to be robust against taphonomic loss of foliar characters and/or taxonomic diversity (Spicer *et al.* 2005, 2011), an accurate knowledge of the taphonomic context is very useful to understand past vegetation and ecology (Burnham 1989; Tosal & Martín-Closas 2016; Tosal *et al.* 2018).

Additionally to proxy data, our results can also be compared to more global climate prediction from available model simulations. Most of the terrestrial climate simulations on Paleocene and Eocene have focused on warm periods such as PETM (Shellito *et al.* 2003; Winguth *et al.* 2010; Jones *et al.* 2013; Lunt *et al.* 2017) and early Eocene (Huber & Sloan 2001; Lunt *et al.* 2012; Lunt *et al.* 2017; Huber & Caballero 2011; Inglis *et al.* 2017). Nevertheless, we were able to compare our results with the HadCM3L model simulations of the Paleocene and Eocene climates from Lunt *et al.* (2016). The temperatures reconstructed for Menat and Gelinden are similar to modeled temperatures for Europe during Selandian (Lunt *et al.* 2016, see online data), while Sézanne temperatures are higher (*c.* 3°) than the simulations for the Thanetian. Similarly, Célas temperatures were higher (*c.* 2.5°) than the simulations for the Priabonian (Lunt *et al.* 2016). Higher data temperatures than model simulations were expected, as models generally produce colder temperatures than proxy data during the greenhouse world period (Huber & Caballero 2011).

As observed by Li *et al.* (2018), MAT and CMMT from fossil leaves during Oligocene (Armissan and Aix-en-Provence) are consistent with model simulation, while WMMT is lower. Late Miocene annual temperature in Saint-Bauzile is quite similar to the ECHAM4/ML simulations in the Northern Hemisphere, though regional differences could exist (Micheels *et al.* 2009).

Discrepancies between data and models can be explained by several factors such as a difference of resolution between data and model; uncertainties in past altitude, topography and paleogeographic position of the fossil localities (Lunt *et al.* 2016; Li *et al.* 2018); bias linked to the proxy itself (Huber & Caballero 2011); the simulated atmospheric CO2 (Micheels *et al.* 2009) and age constraints of the fossil deposit. The discussion of these methodological aspects is beyond the scope of this present study. Nevertheless, future work should focus on the discrepancies between data and model, notably by addressing issues on altitude and geographic position of the fossil localities.

CONCLUSIONS AND PERSPECTIVES

This study provides new quantitative paleoclimate estimates for several key periods of the Cenozoic, in Western Europe. Our results are broadly consistent with previous literature for this region, based on several terrestrial and marine proxies. They suggest: 1) relatively cooler conditions during Paleocene and a gradual increase of MAT and precipitation range during mid- to late Paleocene; 2) increased temperature seasonality rather than a global cooling at the Eocene-Oligocene transition; 3) an increase of temperature between early and late Oligocene; and 4) similar conditions in Western Europe as in other parts of Europe, consistently with the previously observed weak temperature gradient during middle Miocene.

Obviously, these collections do not provide a high-resolution record of the temperature and precipitation during Cenozoic. However, their study documents the climate at several key periods of the Tertiary climatic evolution. The consistency of our results with previous studies based on multiples proxies supports the use of historical collections to reconstruct past climates.

Future steps include complementary studies on the depositional context of these paleoenvironment, thus improving our understanding of the paleofloras. Additionally, the application of Nearest-Living Relative approach, based on taxonomical reinvestigation of these paleofloras, would precise our interpretation of both vegetation types and paleoclimates presented in this study.

Acknowledgements
The authors wish to thank the E-Recolnat infrastructure (ANR-11-INBS-0004) and J. Falconnet for providing photographs of specimens from the Muséum national d'Histoire naturelle; the curators of the Institut royal des Sciences naturelles de Belgique (A. Folie and C. Prestianni), the Muséum d'Histoire naturelle of Marseille and S. Jouve for giving us access to the collections and for their help they provided during the study of these collections. Finally, the authors thank Anita Roth-Nebelsick and an anonymous reviewer for their constructive comments and corrections on the first version of the manuscript.

REFERENCES

Adatte T., Bolle M. P., Kaenel E. D., Gawenda P., Winkler W. & Von Salis K. 2000. — Cimatic evolution from Paleocene to earliest Eocene inferred from clay-minerals: A transect from northern Spain (Zumaya) to southern (Spain, Tunisia) and southeastern Tethys margins (Israel, Negev). *GFF* 122: 7-8. https://doi.org/10.1080/11035890001221007

Akhmetiev M. A., Gavrilov Y. O. & Zaporozhets N. I. 2017. — Events at the turn of the Eocene and Oligocene in the Central Eurasia Region (middle latitudes) *Doklady Earth Sciences* 473: 273-276. https://doi.org/10.1134/S1028334X17030199

Bailey I. W. & Sinnott E. W. 1915. — A Botanical Index of Cretaceous and Tertiary Climates. *Science* 41: 831-834. https://doi.org/10.1126/science.41.1066.831

Bailey I. W. & Sinnott E. W. 1916. — The climatic distribution of certain types of angiosperm leaves. *American Journal of Botany* 3: 24-39. https://www.jstor.org/stable/2435109

Barrick R. E., Fischer A. G., Showers W. J. 1999. — Oxygen isotopes from turtle bone: applications for terrestrial paleoclimates? *Palaios* 14: 186-191. https://www.jstor.org/stable/3515374

Bechtel A., Gratzer R., Sachsenhofer R. F., Gusterhuber J., Lücke A., Püttmann W. 2008. — Biomarker and carbon isotope variation in coal and fossil wood of Central Europe through the Cenozoic. *Palaeogeography, Palaeoclimatology, Palaeoecology* 262: 166-175. https://doi.org/10.1016/j.palaeo.2008.03.005

Böhme M. 2003. — The Miocene Climatic Optimum: evidence from ectothermic vertebrates of Central Europe. *Palaeogeography, Palaeoclimatology, Palaeoecology* 195: 389-401. https://doi.org/10.1016/S0031-0182(03)00367-5

Brice D. 1965. — Recherches sur la flore mio-pliocène de la montagne d'Andance (Coiron-Ardèche). *Annales de la Société géologique du Nord* LXXXV: 189-236.

Brongniart A.-T. 1828a. — Prodrome d'une histoire des végétaux fossilles. Levrault F. G. (eds), Strasbourg, France. https://doi.org/10.5962/bhl.title.62840

Brongniart A.-T. 1828b. — Notice sur les plantes d'Armissan, près Narbonne. *Annales des Sciences naturelles* 15: 43-51.

Bruch A. A., Uhl D. & Mosbrugger V. 2007. — Miocene climate in Europe – Patterns and evolution: A first synthesis of NECLIME. *Palaeogeography, Palaeoclimatology, Palaeoecology* 253: 1-7. https://doi.org/10.1016/j.palaeo.2007.03.030

Bruch A. A., Utescher T. & Mosbrugger V. 2011. — Precipitation patterns in the Miocene of Central Europe and the development of continentality *in* Utescher T., Böhme M., Mosbrugger V. (eds), The Neogene of Eurasia: Spatial gradients and temporal trends - The second synthesis of NECLIME. *Palaeogeography, Palaeoclimatology, Palaeoecology* 304: 202-211. https://doi.org/10.1016/j.palaeo.2010.10.002

Buchardt B. 1977. — Oxygen isotope ratios from shell material from the Danish middle paleocene (Selandian) deposits and their interpretation as paleotemperature indicators. *Palaeogeography, Palaeoclimatology, Palaeoecology* 22: 209-230. https://doi.org/10.1016/0031-0182(77)90029-3

Burnham R. J. 1989. — Relationships between standing vegetation and leaf litter in a paratropical forest: implications for paleobotany. *Review of Palaeobotany and Palynology* 58*:* 5-32. https://doi.org/10.1016/0034-6667(89)90054-7

Collinson M. E. & Hooker J. J. 2003. — Paleogene vegetation of Eurasia: framework for mammalian faunas. *Deinsea* 10: 41-84.

Collinson M. E., Fowler K. & Boulter M. C. 1981. — Floristic changes indicate a cooling climate in the Eocene of southern England. *Nature* 291: 315-317. https://doi.org/10.1038/291315a0

De Bast E. & Smith T. 2017. — The oldest Cenozoic mammal fauna of Europe: implication of the early Palaeocene Hainin reference fauna for mammalian evolution and dispersals during the Palaeocene. *Journal of Systematic Palaeontology* 15: 741-785. https://doi.org/10.1080/14772019.2016.1237582

Demarcq G., Ballesio R., Rage J.-C., Guerin C., Mein P. & Meon H., 1983. — Données paléoclimatiques du Néogène de la Vallée du Rhône (France). *Palaeogeography, Palaeoclimatology, Palaeoecology* 42: 247-272. https://doi.org/10.1016/0031-0182(83)90025-1

Depape G. 1912. — Note sur quelques chênes miocènes et pliocènes. *Revue Générale de Botanique* 24: 355-372.

Dinarès-Turell J., Baceta J. I., Bernaola G., Orue-Etxebarria X. & Pujalte V. 2007. — Closing the Mid-Palaeocene gap: Toward a complete astronomically tuned Palaeocene Epoch and Selandian and Thanetian GSSPs at Zumaia (Basque Basin, W Pyrenees). *Earth and Planetary Science Letters* 262: 450-467. https://doi.org/10.1016/j.epsl.2007.08.008

Domingo L., Lopez-Martinez N., Soler-Gijon R. & Grimes S. T. 2007. — A multi-proxy geochemical investigation of the early Paleocene (Danian) continental palaeoclimate at the Fontllonga-3 site (South Central Pyrenees, Spain). *Palaeogeography, Palaeoclimatology, Palaeoecology*, 256: 71-85. https://doi.org/10.1016/j.palaeo.2007.09.009

Engler A. 1882. — Die extratropischen Gebiete der Südlichen Hemisphäre und die tropischen Gebiete *in* Engelmann W. (eds). *Versuch einer Entwicklungsgeschichte der Pflanzenwelt, insbesondere der Florengebiete seit der Tertiärperiode,* vol. 2. Leipzig, Germany.

Fan M., Ayyash S. A., Tripati A., Passey B. H. & Griffith E. M. 2018. — Terrestrial cooling and changes in hydroclimate in the continental interior of the United States across the Eocene-Oligocene boundary. *GSA Bulletin* 130: 1073-1084. https://doi.org/10.1130/B31732.1

Feist-Castel M. 1971. — Sur les Charophytes fossiles du bassin Tertiaire d'Ales (Gard). *Geobios* 4: 157-172. https://doi.org/10.1016/S0016-6995(71)80014-1

Flower B. P. & Chisholm K. E. 2006. — Magnetostratigraphic calibration of the late Oligocene climate transition *in* Tiedmann R., Mix A. C., Richter C. & Ruddiman W. F. (eds), *Proceedings of the Ocean Drilling Program: Scientific Results* 202: 1-15. https://doi.org/10.2973/odp.proc.sr.202.204.2006

Flower B. P. & Kennett J. P. 1994. — The middle Miocene climatic transition: East Antarctic ice sheet development, deep ocean circulation and global carbon cycling. *Palaeogeography, palaeoclimatology, palaeoecology* 108: 537-555. https://doi.org/10.1016/0031-0182(94)90251-8

Fontannes F. 1885. — Le groupe d'Aix dans le Dauphiné, la Provence et le Bas-Languedoc *in* Études stratigraphiques et paléontologiques pour servir à l'histoire de la période tertiaire dans le bassin du Rhône, partie VIII. Georg, Lyon.

Freytet P., Duringer P., Koeniguer J.-C., Lablanche G., Laurain M. & Pons D. 2001. — Distribution and paleoecology of freshwater algae and stromatolites: IV, some examples from the Tertiary of the Parisian Basin and the Alsace Graben (France). *Annales de Paléontologie* 87: 143-205. https://doi.org/10.1016/S0753-3969(01)80009-4

Gaudant J., Nel A., Nury D., Veran M. & Carnevale G. 2017. — The uppermost Oligocene of Aix-en-Provence (Bouches-du-Rhône, Southern France): A Cenozoic brackish subtropical *Konservat-Lagerstätte*, with fishes, insects and plants. *Comptes Rendus Palevol* 17: 460-478. https://doi.org/10.1016/j.crpv.2017.08.002

Gehler A., Gingerich P. D. & Pack A. 2016. — Temperature and atmospheric CO2 concentration estimates through the PETM using triple oxygen isotope analysis of mammalian bioapatite. *Proceedings of the National Academy of Sciences* 113: 7739-7744. https://doi.org/10.1073/pnas.1518116113

Gingerich P. D. 2000. — Paleocene/Eocene boundary and continental vertebrate faunas of Europe and North America. *GFF* 122: 57-59. https://doi.org/10.1080/11035890001221057

Gregory-Wodzicki K. M. 2000. — Relationships between leaf morphology and climate, Bolivia: implications for estimating paleoclimate from fossil floras. *Paleobiology* 26: 668-688. https://doi.org/10.1666/0094-8373(2000)026<0668:RBLMAC>2.0.CO;2

Greenwood D. R., Wilf P., Wing S. L. & Christophel D. C. 2004. — Paleotemperature estimation using leaf-margin analysis: is Australia different? *Palaios* 19 (2): 129-142. https://doi.org/10.1669/0883-1351(2004)019<0129:PEULAI>2.0.CO;2

Grimes S. T., Hooker J. J., Collinson M. E. & Mattey D. P. 2005. — Summer temperatures of late Eocene to early Oligocene freshwaters. *Geology* 33: 189-192. https://doi.org/10.1130/G21019.1

Hamer J. M. M., Sheldon N. D. & Nichols G. J. 2007. — Global Aridity during the Early Miocene? A Terrestrial Paleoclimate Record from the Ebro Basin, Spain. *The Journal of Geology* 115: 601-608. http://www.jstor.org/stable/10.1086/519780

Hao H., Ferguson D. K., Feng G. P., Ablaev A., Wang Y. F. & Li C. S. 2010. — Early Paleocene vegetation and climate in Jiayin, NE China. *Climatic Change* 99: 547-566. https://doi.org/10.1007/s10584-009-9728-6

Héran M.-A., Lecuyer C. & Legendre S. 2010. — Cenozoic long-term terrestrial climatic evolution in Germany tracked by δ18O of rodent tooth phosphate. *Palaeogeography, Palaeoclimatology, Palaeoecology* 285: 331-342. https://doi.org/10.1016/j.palaeo.2009.11.030

Herman A. B. & Spicer R. A. 1997. — New quantitative palaeoclimate data for the Late Cretaceous Arctic: evidence for a warm polar ocean. *Palaeogeography, Palaeoclimatology, Palaeoecology* 128: 227-251. https://doi.org/10.1016/S0031-0182(96)00080-6

Hollis C. J., Taylor K. W., Handley L., Pancost R. D., Huber M., Creech J. B. & Gibbs S. 2012. — Early Paleogene temperature history of the Southwest Pacific Ocean: Reconciling proxies and models. *Earth and Planetary Science Letters* 349: 53-66. https://doi.org/10.1016/j.epsl.2012.06.024

Hollis C. J., Tayler M. J. S., Andrew B., Taylor K. W., Lurcock P., Bijl P. K., Kulhanek D. K., Crouch E. M., Nelson C. S., Pancost R. D., Huber M., Wilson G. S., Ventura G. T., Crampton J. S., Schiøler P. & Phillips A. 2014. — Organic-rich sedimentation in the South Pacific Ocean associated with Late Paleocene climatic cooling. *Earth-Science Reviews* 134: 81-97. https://doi.org/10.1016/j.earscirev.2014.03.006

Hooyberghs H., Jutson D. & Moorkens T. 2001. — Microfossils of the Heers Formation (Middle Paleocene) of NE Belgium: Biostratigraphy, depositional and climatic-hydrographic setting *in* Vandenberghe N. (eds), Contributions to the Paleogene and Neogene Stratigraphy of the North Sea Basin: Proceedings of the 7th Biannual Meeting of the Regional Committees of Northern Neogene and Paleogene Stratigraphy. *Aardkundige Mededelingen* 11: 29-44.

Hren M. T., Sheldon N. D., Grimes S. T., Collinson M. E., Hooker J. J., Bugler M. & Lohmann K. C. 2013. — Terrestrial cooling in Northern Europe during the Eocene–Oligocene transition. *Proceedings of the National Academy of Sciences of the United States of America* 110: 7562-7567. https://doi.org/10.1073/pnas.1210930110

Huber M. & Caballero R. 2011. — The early Eocene equable climate problem revisited. *Climate of the Past* 7: 603-633. https://doi.org/10.5194/cp-7-603-2011

Huber M. & Sloan L. C. 2001. — Heat transport, deep waters, and thermal gradients: Coupled simulation of an Eocene greenhouse climate. *Geophysical Research Letters* 28: 3481-3484. https://doi.org/10.1029/2001GL012943

Huyghe D., Lartaud F., Emmanuel L., Merle D. & Renard M. 2015. — Palaeogene climate evolution in the Paris Basin from oxygen stable isotope (Δ18O) compositions of marine molluscs. *Journal of the Geological Society* 172: 576-587. https://doi.org/10.1144/jgs2015-016

Huyghe D., Emmanuel L., Renard M., Lartaud F., Génot P., Riveline J.& Merle D. 2017. — Significance of shallow-marine and non-marine algae stable isotope (δ18O) compositions over long periods: Example from the Palaeogene of the Paris Basin. *Palaeogeography, Palaeoclimatology, Palaeoecology* 485: 247-259. https://doi.org/10.1016/j.palaeo.2017.06.017

Inglis G. N., Collinson M. E., Riegel W., Wilde V., Farnsworth A., Lunt D. J. & Naafs B. D. A. 2017. — Mid-latitude continental temperatures through the early Eocene in western Europe. *Earth and Planetary Science Letters* 460: 86-96. https://doi.org/10.1016/j.epsl.2016.12.009

Iskandar D. 1990. — La diatomite Miocène de la montagne d'Andance, carrière de Saint-Bauzile (Ardèche, France): étude palynologique, écostratigraphie, paléoclimatologie. Département des sciences de la terre, Université Claude-Bernard, Lyon.

Ivany L. C., Patterson W. P. & Lohmann K. C. 2000. — Cooler winters as a possible cause of mass extinctions at the Eocene/Oligocene boundary. *Nature* 407: 887-890. https://doi.org/10.1038/35038044

JACQUES F. M. B., SU T., SPICER R. A., XING Y., HUANG Y., WANG W. & ZHOU Z. 2011. — Leaf physiognomy and climate: Are monsoon systems different? *Global and Planetary Change* 76: 56-62. https://doi.org/10.1016/j.gloplacha.2010.11.009

JONES T. D., LUNT D. J., SCHMIDT D. N., RIDGWELL A., SLUIJS A., VALDES P. J. & MASLIN M. 2013. — Climate model and proxy data constraints on ocean warming across the Paleocene–Eocene Thermal Maximum. *Earth-Science Reviews* 125: 123-145. https://doi.org/10.1016/j.earscirev.2013.07.004

KENNEDY E. M., SPICER R. A. & REES P. M. 2002. — Quantitative palaeoclimate estimates from Late Cretaceous and Paleocene leaf floras in the northwest of the South Island, New Zealand. *Palaeogeography, Palaeoclimatology, Palaeoecology* 184: 321-345. https://doi.org/10.1016/S0031-0182(02)00261-4

KENNEDY E. M., ARENS N. C., REICHGELT T., SPICER R. A., SPICER T. E. V., STRANKS L. & YANG J. 2014. — Deriving temperature estimates from Southern Hemisphere leaves. *Palaeogeography, Palaeoclimatology, Palaeoecology* 412: 80-90. https://doi.org/10.1016/j.palaeo.2014.07.015

KENNETT J. P. & SHACKLETON N. J. 1976. — Oxygen isotopic evidence for the development of the psychrosphere 38 Myr ago. *Nature* 260: 513-515. https://doi.org/10.1038/260513a0

KENNETT J. P. & STOTT L. D. 1991. — Abrupt deep-sea warming, palaeoceanographic changes and benthic extinctions at the end of the Palaeocene. *Nature* 353: 225-229. https://doi.org/10.1038/353225a0

KHAN M. A., SPICER R. A., BERA S., GHOSH R., YANG J., SPICER T. E. V., GUO S., SU T., JACQUES F. M. B. & GROTE P. J. 2014. — Miocene to Pleistocene floras and climate of the Eastern Himalayan Siwaliks, and new palaeoelevation estimates for the Namling–Oiyug Basin, Tibet. *Global and Planetary Change* 113: 1-10. https://doi.org/10.1016/j.gloplacha.2013.12.003

KOCH B. E. 1963. — Fossil plants from the lower Paleocene of the Agatdalen (Angmârtussut) area, central Nûgssuaq peninsula, northwest Greenland. *Meddel Grønland* 172: 1-175.

KOCH P. L., ZACHOS J. C. & GINGERICH P. D. 1992. — Correlation between isotope records in marine and continental carbon reservoirs near the Palaeocene/Eocene boundary. *Nature* 358: 319-322. https://doi.org/10.1038/358319a0

KUNZMANN L., MORAWECK K., MÜLLER C., SCHRÖDER I., WAPPLER T., GREIN M. & ROTH-NEBELSICK A. 2018. — A Paleogene leaf flora (Profen, Sachsen-Anhalt, Germany) and its potentials for palaeoecological and palaeoclimate reconstructions. *Flora* https://doi.org/10.1016/j.flora.2018.11.005.

KÜRSCHNER W. M. & KVAČEK Z. 2009. — Oligocene-Miocene CO2 fluctuations, climatic and palaeofloristic trends inferred from fossil plant assemblages in central Europe. *Bulletin of Geosciences* 84: 189-202.

KVAČEK Z. 2010. — Forest flora and vegetation of the European early Palaeogene–a review. *Bulletin of Geoscience* 85: 3-16.

KVAČEK Z. 2002a. — Novelties on *Doliostrobus* (Doliostrobaceae), an extinct conifer genus of the European Palaeogene. *Časopis Národního Muzea* 171: 131-175.

KVAČEK Z. 2002b. — (1568) Proposal to conserve the name *Doliostrobus* Marion (1888)(fossil Pinopsida) against *Doliostrobus* Marion (1884)(fossil Lycopsida). *Taxon* 51: 820-821. https://www.jstor.org/stable/1555054

LANGERON M. 1899. — Contributions à l'étude de la flore fossil de Sézanne. *Bulletin de la Société d'Histoire naturelle d'Autun*, tome 12.

LAPPARENT A. F. DE 1906. — *Traité de Géologie* (5 éd.). G. Masson, Paris.

LAPPARENT A. F. DE 1938. — Études de Paléontologie stratigraphique sur les faunes continentales de Provence. *Mémoires de la Société géologique de France* 35: 580.

LAURAIN M. & MEYER R. 1986. — Stratigraphie et paléogéographie de la base du Paléogène champenois. *Géologie de la France* 1: 103-123.

LAURENT L. 1899 — Flore des calcaires de Célas. *Annales du Musée d'histoire naturelle de Marseille*. Série II, Tome I. Mouillot, Marseille, 148 p.

LAURENT L. 1912. — Flore fossile des schistes de Menat (Puy-de-Dôme). *Annales du Musée d'Histoire naturelle de Marseille*, Tome XIV. Mouillot, Marseille, 216 p.

LAVOCAT R. 1955. — Sur un squelette de *Pseudosciurus* provenant du gisement d'Armissan Aude. *Annales de Paléontologie* 51: 77-89.

LECOQ H. 1829. — Description géologique du bassin de Menat. *Annales scientifiques, littéraires et industrielles de l'Auvergne* 2: 433-447.

LETTÉRON A., HAMON Y., FOURNIER F., SERANNE M., PELLENARD P. & JOSEPH P. 2018. — Reconstruction of a saline, lacustrine carbonate system (Priabonian, St-Chaptes Basin, SE France): Depositional models, paleogeographic and paleoclimatic implications. *Sedimentary Geology* 367: 20-47. https://doi.org/10.1016/j.sedgeo.2017.12.023

LI S., XING Y., VALDES P. J., HUANG Y., SU T., FARNSWORTH A., LUNT D. J., TANG H., KENNEDY A. T. & ZHOU Z. 2018. — Oligocene climate signals and forcings in Eurasia revealed by plant macrofossil and modelling results. *Gondwana Research* 61: 115-127. https://doi.org/10.1016/j.gr.2018.04.015

LIU Z., PAGANI M., ZINNIKER D., DECONTO R., HUBER M., BRINKHUIS H., SHAH S. R., LECKIE R. M. & PEARSON A. 2009. — Global Cooling During the Eocene-Oligocene Climate Transition. *Science* 323: 1187-1190. https://doi.org/10.1126/science.1166368

LUNT D. J., DUNKLEY JONES T., HEINEMANN M., HUBER M., LEGRANDE A., WINGUTH A. & VALDES P. 2012. — A model–data comparison for a multi-model ensemble of early Eocene atmosphere–ocean simulations: EoMIP. *Climate of the Past* 8: 1717-1736. https://doi.org/10.5194/cp-8-1717-2012

LUNT D. J., FARNSWORTH A., LOPTSON C., FOSTER G. L., MARKWICK P., O'BRIEN C. L., PANCOST R. D., ROBINSON S. A. & WROBEL N. 2016. — Palaeogeographic controls on climate and proxy interpretation. *Climate of the Past* 12: 1181-1198. https://doi.org/10.5194/cp-12-1181-2016

LUNT D. J., HUBER M., ANAGNOSTOU E., BAATSEN M. L., CABALLERO R., DECONTO R. & FOSTER G. L. 2017. — The DeepMIP contribution to PMIP4: experimental design for model simulations of the EECO, PETM, and pre-PETM (version 1.0). *Geoscientific Model Development* 10: 889-901. https://doi.org/10.5194/gmd-10-889-2017

MAI D. H. 1989. — Development and regional differentiation of the European vegetation during the Tertiary, in EHRENDORFER F. (eds), *Woody Plants – Evolution and Distribution since the Tertiary*. Springer, Vienna: 79-91. https://doi.org/10.1007/978-3-7091-3972-1_4

MAI D. H. 1991. — Palaeofloristic changes in Europe and the confirmation of the Arctotertiary-Palaeotropical geofloral concept. *Review of Palaeobotany and Palynology* 68: 29-36. https://doi.org/10.1016/0034-6667(91)90055-8.

MAI D. H. 1995. — Tertiäre Vegetationsgeschichte Europas. Methoden und Ergebnisse. *Feddes Repert* 106: 331.

MARION A. F. 1888. — *Doliostrobus sternbergii* – Nouveau genre de conifères fossiles. *Annales des Sciences Géologiques* 20: 1-20.

MARTY P. 1903. — Flore miocène de Joursac (Cantal). Revue de la Haute-Auvergne 5: 1-92.

MATHERON P. 1862. — Recherches comparatives sur les dépôts fluvio-lacustres tertiaires des environs de Montpellier, de l'Aude et de la Provence. Arnaud, Marseille, 112p.

MCINERNEY F. A. & WING S. L. 2011. — The Paleocene-Eocene Thermal Maximum: A perturbation of carbon cycle, climate, and biosphere with implications for the future. *Annual Review of Earth and Planetary Sciences* 39: 489-516. https://doi.org/10.1146/annurev-earth-040610-133431

MÉTAIS G. & SEN S. 2018. — The late Miocene mammals from the Konservat-Lagerstätte of Saint-Bauzile (Ardèche, France). *Comptes Rendus Palevol* 17 (7): 479-493. https://doi.org/10.1016/j.crpv.2018.05.001

MICHEELS A., BRUCH A. A. & MOSBRUGGER V. 2009. — Miocene Climate Modelling Sensitivity Experiments for Different CO2 Concentrations. *Palaeontologia Electronica* 12: 1-19. http://palaeo-electronica.org/2009_2/172/index.html

MOISEEVA M. G., KODRUL T. M. & HERMAN A. B. 2018. — Early Paleogene Boguchan flora of the Amur Region (Russian Far East): Composition, age and palaeoclimatic implications. *Review of Palaeobotany and Palynology* 253: 15-36. https://doi.org/10.1016/j.revpalbo.2018.03.003

MOSBRUGGER V. & UTESCHER T. 1997. — The coexistence approach—a method for quantitative reconstructions of Tertiary terrestrial palaeoclimate data using plant fossils. *Palaeogeography, Palaeoclimatology, Palaeoecology* 134: 61-86. https://doi.org/10.1016/S0031-0182(96)00154-X

MOSBRUGGER V., UTESCHER T. & DILCHER D. L. 2005. — Cenozoic continental climatic evolution of Central Europe. *Proceedings of the National Academy of Sciences* 102: 14964-14969. https://doi.org/10.1073/pnas.0505267102

MOUTON J. A. 1970. — Florule élémentaire du Thanétien de Sézanne. *Comptes Rendus Du Congrès National Des Sociétés Savantes: Section Des Sciences* 3: 213-225.

NAAFS B. D. A., ROHRSSEN M., INGLIS G. N., LÄHTEENOJA O., FEAKINS S. J., COLLINSON M. E., KENNEDY E. M., SINGH P. K., SINGH M. P., LUNT D. J. & PANCOST R. D. 2018. — High temperatures in the terrestrial mid-latitudes during the early Palaeogene. *Nature Geoscience* 11: 766-771. https://doi.org/10.1038/s41561-018-0199-0

NURY D. 1990. — L'Oligocène de Provence méridionale: stratigraphie, dynamique sédimentaire, reconstitutions paléographiques. Documents du BRGM, Editions du BRGM, BRGM, Orléans, France.

PANCOST R. D., TAYLOR K. W. R., INGLIS G. N., KENNEDY E. M., HANDLEY L., HOLLIS C. J., CROUCH E. M., PROSS J., HUBER M., SCHOUTEN S., PEARSON P. N., MORGANS H. E. G. & RAINE J. I. 2013. — Early Paleogene evolution of terrestrial climate in the SW Pacific, Southern New Zealand. *Geochemistry, Geophysics, Geosystems* 14: 5413-5429. https://doi.org/10.1002/2013GC004935

PASTRE J.-F., SINGER B. S., GUILLOU H., PUPIN J.-P. & RIOU B. 2004. — Chronostratigraphy of the key Upper Miocene (Lower Turolian) sequence of la Montagne d'Andance (Ardèche, France). Implications of new 40Ar/39Ar laser fusion and unspiked K-Ar dating of trachytic tephra and basalts. *Bulletin de la Société Géologique de France* 17: 3-10. https://doi.org/10.2113/175.1.3

PEPPE D. J., BAUMGARTNER A., FLYNN A. & BLONDER B. 2018. — Reconstructing paleoclimate and paleoecology using fossil leaves *in* CROFT D. A., SU D. & SIMPSON S. (eds), *Methods in Paleoecology*. Springer, Cham. https://doi.org/10.1007/978-3-319-94265-0_13

PITON L. E. 1940. — Paléontologie du gisement Éocene de Menat. Vallier, Clermont-Ferrand, France, 303p.

POUND M. J. & SALZMANN U. 2017. — Heterogeneity in global vegetation and terrestrial climate change during the late Eocene to early Oligocene transition. *Scientific Reports* 7: 43386. https://doi.org/10.1038/srep43386

PROSS J., BRUCH A. A., MOSBRUGGER V. & KVAČEK Z. 2001. — Paleogene pollen and spores as a tool for quantitative paleoclimate reconstructions: the Rupelian (Oligocene) of Central Europe, *in* GOODMAN D. K. & CLARKE R. T. (eds), *Proceedings of the IX International Palynological Congress*. Houston, TX, USA: 299-310.

REMY J.-A. 1985. — Nouveaux gisements de mammifères et reptiles dans les Grès de Célas (Eocène sup. du Gard). Etude des Palaeotheriidés (Perissodactyla, Mammalia). *Palaeontographica A* 189: 171-225.

REMY J.-A. 1994. — Une faunule de vertébrés sous la base des Grès de Célas (Eocène sup.) à Saint-Dézéry (Gard). *Palaeovertebrata* 23: 211-216.

RÖGL F. 1999. — Mediterranean and Paratethys. Facts and hypotheses of an Oligocene to Miocene paleogeography (short overview). *Geologica Carpathica* 5: 339-349.

ROIRON P. 1992. — Flores, végétations et climats du Néogène méditerranéen: apports de macroflores du Sud de la France et du Nord-Est de l'Espagne. Université de Montpellier 2.

SAPORTA G. DE 1863. — Étude sur la végétation du sud-est de la France à l'époque tertiaire. Première partie. *Annales des sciences naturelles, Botanique* Tome XVII, 4ème série: 49-140.

SAPORTA G. DE 1865. — Étude sur la végétation de sud-est de la France á l'époque tertiaire. Deuxième partie, III: Flore d'Armissan et de Peyriac dans le bassin de Narbonne (Aude). *Annales des sciences naturelles, Botanique* Tome XV, 5ème série.

SAPORTA G. DE 1868. — Prodrome d'une flore fossile des travertins anciens de Sézanne. *Mémoires de la Société Géologique de France* 8: 289-437.

SAPORTA G. DE 1872. — Étude sur la végétation du sud-est de la France à l'époque tertiaire. Supplément I : Révision de la flore des gypses d'Aix. *Annales des sciences naturelles, Botanique* Tome XV, 5ème série.

SAPORTA G. DE 1879. — Le monde des Plantes avant l'apparition de l'Homme. G. Masson, Paris.

SAPORTA G. DE 1888a. — Dernières adjonctions à la flore fossile d'Aix-en-Provence. *Annales des sciences naturelles, Botanique* Tome XVII, 7e série.

SAPORTA G. DE 1888b. — Notions stratigraphiques et paléontologiques appliquées à l'étude du gisement des plantes fossiles d'Aix. *Annales de la Société Géologique de France* 20: 1-60.

SAPORTA G. DE & MARION A. F. 1873. — *Essai sur l'état de la végétation à l'époque des marnes heersiennes de Gelinden*. F. Hayez, Bruxelles, 112p.

SAPORTA G. DE & MARION A. F. 1878. — *Révision de la flore heersienne de Gelinden: d'après une collection appartenant au comte G. de Looz*. Académie royale des sciences, des lettres et des beaux-arts de Belgique, Bruxelles.

SAPORTA G. DE & MARION A. F. 1885. — *L'évolution du règne végétal: les phanérogames*. G. Baillière, Paris, 238 p.

SCHMIDT-KITTLER N. 1971. — Odontologische Untersuchungen an Pseudosciuriden (Rodentia, Mammalia) des Alttertiärs: mit 8 Tabellen. Bayer. *Abhandlungen der Bayerischen Akademie der Wissenschaften* 150: 1-133.

SCHMITZ B. & PUJALTE V. 2007. — Abrupt increase in seasonal extreme precipitation at the Paleocene-Eocene boundary. *Geology* 35: 215-218. https://doi.org/10.1130/G23261A.1

SHELLITO C. J., SLOAN L. C. & HUBER M. 2003. — Climate model sensitivity to atmospheric CO2 levels in the Early–Middle Paleogene. *Palaeogeography, Palaeoclimatology, Palaeoecology* 193: 113-123. https://doi.org/10.1016/S0031-0182(02)00718-6

SOKAL R. R. & SNEATH P. H. A. 1963 — Principles of numerical taxonomy. Freeman, San Francisco, 359 p.

SONG Y., WANG Q., AN Z., QIANG X., DONG J., CHANG H., ZHANG M. & GUO X. 2017. — Mid-Miocene climatic optimum: clay mineral evidence from the red clay succession, Longzhong Basin, Northern China. *Palaeogeography, Palaeoclimatology, Palaeoecology* 512: 46-55. https://doi.org/10.1016/j.palaeo.2017.10.001

SPEIJER R. P. 2003. — Danian-Selandian sea-level change and biotic excursion on the southern Tethyan margin (Egypt). *Geological Society of America Special Papers* 369: 275-290.

SPICER R. A., HERMAN A. B. & KENNEDY E. M. 2005. — The sensitivity of CLAMP to taphonomic loss of foliar physiognomic characters. *Palaios* 20: 429-438. https://doi.org/10.2110/palo.2004.P04-63

SPICER R. A., VALDES P. J., SPICER T. E. V., CRAGGS H. J., SRIVASTAVA G., MEHROTRA R. C. & YANG J. 2009. — New developments in CLAMP: calibration using global gridded meteorological data. *Palaeogeography, Palaeoclimatology, Palaeoecology* 283: 91-98. https://doi.org/10.1016/j.palaeo.2009.09.009

SPICER R. A., BERA S., DE BERA S., SPICER T. E. V., SRIVASTAVA G., MEHROTRA R. & YANG J. 2011. — Why do foliar physiognomic climate estimates sometimes differ from those observed? Insights from taphonomic information loss and a CLAMP case study from

the Ganges Delta. *Palaeogeography, Palaeoclimatology, Palaeoecology* 302: 381-395. https://doi.org/10.1016/j.palaeo.2011.01.024

STOCKMANS F. 1960. — Initiation à la paléobotanique stratigraphique de la Belgique et notions connexes. Institut Royal des Sciences Naturelles de Belgique, Bruxelles.

STOCKMANS F. 1932. — Sur des épidermes de dicotylédonées (*Dewalquea gelindenensis* Saporta et Marion et *Litsea elatinervis* Saporta et Marion) des marnes de Gelinden (Paléocène). Institut Royal des Sciences Naturelles de Belgique, Bruxelles.

TEODORIDIS V., MAZOUCH P., SPICER R. A. & UHL D. 2011. — Refining CLAMP – investigations towards improving the Climate Leaf Analysis Multivariate Program. *Palaeogeography, Palaeoclimatology, Palaeoecology* 299: 39-48. https://doi.org/10.1016/j.palaeo.2010.10.031

TER BRAAK C. J. 1986. — Canonical correspondence analysis: a new eigenvector technique for multivariate direct gradient analysis. *Ecology* 67: 1167-1179. https://doi.org/10.2307/1938672

TOSAL A. & MARTÍN-CLOSAS C. 2016. — Taphonomy and palaeoecology of the Oligocene flora from Cervera (Catalonia, Spain) and their implication in palaeoclimatic reconstruction. *Review of Palaeobotany and Palynology* 233: 93-103. https://doi.org/10.1016/j.revpalbo.2016.06.008

TOSAL A., SANJUAN J., CARTANYÀ J. & MARTÍN-CLOSAS C. 2018. — Taphonomy and palaeoecology of the uppermost Eocene flora from Sarral (Eastern Ebro Basin): Palaeoclimatic implications. *Palaeogeography, Palaeoclimatology, Palaeoecology* 497: 66-81. https://doi.org/10.1016/j.palaeo.2018.02.006

TRAISER C., KLOTZ S., UHL D. & MOSBRUGGER V. 2005. — Environmental signals from leaves – a physiognomic analysis of European vegetation. *New Phytologist* 166: 465-484. https://doi.org/10.1111/j.1469-8137.2005.01316.x

TRAISER C., ROTH-NEBELSICK A., GREIN M., KOVAR-EDER J., KUNZMANN L., MORAWECK K., LANGE J., KVAČEK J., NEINHUIS C., FOLIE A., DE FRANCESCHI D., KROH A., PRESTIANNI C., POSCHMANN M. & WUTTKE M. 2018. — MORPHYLL: A database of fossil leaves and their morphological traits. *Palaeontologia Electronica* 21.1.1T: 1-17 https://doi.org/10.26879/773

UHL D. & HERRMANN M. 2010. — Palaeoclimate estimates for the Late Oligocene taphoflora of Enspel (Westerwald, West Germany) based on palaeobotanical proxies. *Palaeobiodiversity and Palaeoenvironments* 90: 39-47. https://doi.org/10.1007/s12549-009-0018-0

UHL D., MOSBRUGGER V., BRUCH A. & UTESCHER T. 2003. — Reconstructing palaeotemperatures using leaf floras–case studies for a comparison of leaf margin analysis and the coexistence approach. *Review of Palaeobotany and Palynology* 126 (1-2): 49-64. https://doi.org/10.1016/S0034-6667(03)00058-7

UHL D., BRUCH A. A., TRAISER C. & KLOTZ S. 2006. — Palaeoclimate estimates for the Middle Miocene Schrotzburg flora (S Germany): a multi-method approach. *International Journal of Earth Sciences (Geol Rundsch)* 95: 1071-1085. https://doi.org/10.1007/s00531-006-0083-9

UTESCHER T., BRUCH A. A., MICHEELS A., MOSBRUGGER V. & POPOVA S. 2011. — Cenozoic climate gradients in Eurasia – a palaeo-perspective on future climate change?, *in* UTESCHER T., BÖHME M. & MOSBRUGGER V. (eds), The Neogene of Eurasia: Spatial gradients and temporal trends – The second synthesis of NECLIME. *Palaeogeography, Palaeoclimatology, Palaeoecology* 304: 351-358. https://doi.org/10.1016/j.palaeo.2010.09.031

UTESCHER T., ERDEI B., HABLY L. & MOSBRUGGER V. 2017. — Late Miocene vegetation of the Pannonian Basin *in* Reconstructing Cenozoic vegetation from proxy data and models – a NECLIME synthesis. *Palaeogeography, Palaeoclimatology, Palaeoecology* 467: 131-148. https://doi.org/10.1016/j.palaeo.2016.02.042

VANDENBERGHE N., VAN SIMAEYS S., STEURBAUT E., JAGT J. W. M. & FELDER P. J. 2004. — Stratigraphic architecture of the Upper Cretaceous and Cenozoic along the southern border of the North Sea Basin in Belgium. *Netherlands Journal of Geosciences* 83: 155-171. https://doi.org/10.1017/S0016774600020229

VASSEUR G. 1897. — Note préliminaire sur la constitution géologique du bassin tertiaire d'Aix-en-Provence. *Annales de la Faculté des Sciences de Marseille* 8: 163-172.

VINCENT P. M., AUBERT M., BOIVIN P., CANTAGREL J. M. & LENAT J. F. 1977. — Découverte d'un volcanisme paléocene en Auvergne; les maars de Menat et leurs annexes, étude géologique et géophysique. *Bulletin de la Société Géologique de France* S7-XIX: 1057-1070. https://doi.org/10.2113/gssgfbull.S7-XIX.5.1057

WAPPLER T., CURRANO E. D., WILF P., RUST J. & LABANDEIRA C. C. 2009. — No post-Cretaceous ecosystem depression in European forests? Rich insect-feeding damage on diverse middle Palaeocene plants, Menat, France. *Proceedings of the Royal Society of London B: Biological Sciences* 276: 4271-4277. https://doi.org/10.1098/rspb.2009.1255

WEDMANN S., UHL D., LEHMANN T., GARROUSTE R., NEL A., GOMEZ B., SMITH K. & SCHAAL S. F. K. 2018. — The Konservat-Lagerstätte Menat (Paleocene; France) – an overview and new insights. *Geologica Acta* 16: 189-213. https://doi.org/10.1344/GeologicaActa2018.16.2.5

WILF P. 2000. — Late Paleocene-early Eocene climate changes in southwestern Wyoming: Paleobotanical analysis. *GSA Bulletin* 112: 292-307. https://doi.org/cbc5jb

WILF P., WING S. L., GREENWOOD D. R. & GREENWOOD C. L. 1998. — Using fossil leaves as paleoprecipitation indicators: an Eocene example. *Geology* 26: 203-206. https://doi.org/c38qts

WING S. L., HARRINGTON G. J., SMITH F. A., BLOCH J. I., BOYER D. M. & FREEMAN K. H. 2005. — Transient floral change and rapid global warming at the Paleocene-Eocene boundary. *Science* 310: 993-996. https://doi.org/10.1126/science.1116913

WING S. L., HERRERA F., JARAMILLO C. A., GÓMEZ-NAVARRO C., WILF P. & LABANDEIRA C. C. 2009. — Late Paleocene fossils from the Cerrejón Formation, Colombia, are the earliest record of Neotropical rainforest. *Proceedings of the National Academy of Sciences of the United States of America* 106: 18627-18632. https://doi.org/10.1073/pnas.0905130106

WINGUTH A., SHELLITO C., SHIELDS C. & WINGUTH C. 2010. — Climate response at the Paleocene–Eocene thermal maximum to greenhouse gas forcing – a model study with CCSM3. *Journal of Climate* 23: 2562-2584. https://doi.org/10.1175/2009JCLI3113.1

WOLFE J. A. 1995. — Paleoclimatic Estimates from Tertiary Leaf Assemblages. *Annual Review of Earth and Planetary Sciences* 23: 119-142.

WOLFE J. A. 1980. — Tertiary climates and floristic relationships at high latitudes in the northern hemisphere. *Palaeogeography, Palaeoclimatology, Palaeoecology* 30: 313-323. https://doi.org/10.1016/0031-0182(80)90063-2

WOLFE J. A. 1993. — A method of obtaining climatic parameters from leaf assemblages. *US Geological Survey Bulletin*, vol. 2040.

WOLFE J. A. 1994. — Tertiary climatic changes at middle latitudes of western North America. *Palaeogeography, Palaeoclimatology, Palaeoecology* 108: 195-205. https://doi.org/10.1016/0031-0182(94)90233-X

XING Y., UTESCHER T., JACQUES F. M. B., SU T., LIU Y. C., HUANG Y. & ZHOU Z. 2012. — Paleoclimatic estimation reveals a weak winter monsoon in southwestern China during the late Miocene: evidence from plant macrofossils. *Palaeogeography, Palaeoclimatology, Palaeoecology* 358: 19-26. https://doi.org/10.1016/j.palaeo.2012.07.011

YANG J., WANG Y.-F., SPICER R. A., MOSBRUGGER V., LI C.-S. & SUN Q.-G. 2007. — Climatic reconstruction at the Miocene Shanwang basin, China, using leaf margin analysis, CLAMP, coexistence approach, and overlapping distribution analysis. *American Journal of Botany* 94: 599-608. https://doi.org/10.3732/ajb.94.4.599

YANG J., SPICER R. A., SPICER T. E. V. & LI C.-S. 2011. — 'CLAMP Online': a new web-based palaeoclimate tool and its application to the terrestrial Paleogene and Neogene of North America. *Palaeobiodiversity and Palaeoenvironments* 91: 163. https://doi.org/10.1007/s12549-011-0056-2

YANG J., SPICER R. A., SPICER T. E. V., ARENS N. C., JACQUES F. M. B., SU T., KENNEDY E. M., HERMAN A. B., STEART D. C. & SRIVASTAVA G. 2015. — Leaf form–climate relationships on the global stage: an ensemble of characters. *Global Ecology and Biogeography* 24: 1113-1125. https://doi.org/10.1111/geb.12334

ZACHOS J. C., QUINN T. M. & SALAMY K. A. 1996. — High-resolution (104 years) deep-sea foraminiferal stable isotope records of the Eocene-Oligocene climate transition. *Paleoceanography* 11: 251-266. https://doi.org/10.1029/96PA00571

ZACHOS J. C., PAGANI M., SLOAN L., THOMAS E. & BILLUPS K. 2001. — Trends, rhythms, and aberrations in global climate 65 Ma to present. *Science* 292: 686-693. https://doi.org/10.1126/science.1059412

ZACHOS J. C., WARA M. W., BOHATY S., DELANEY M. L., PETRIZZO M. R., BRILL A., BRALOWER T. J. & PREMOLI-SILVA I. 2003. — A transient rise in tropical sea surface temperature during the Paleocene-Eocene thermal maximum. *Science* 302: 1551-1554. https://doi.org/10.1126/science.1090110

ZACHOS J. C., DICKENS G. R. & ZEEBE R. E. 2008. — An early Cenozoic perspective on greenhouse warming and carbon-cycle dynamics. *Nature* 451: 279-283. https://doi.org/10.1038/nature06588

ZHANG L., WANG C., LI X., CAO K., SONG Y., HU B., LU D., WANG Q., DU X. & CAO S. 2016. — A new paleoclimate classification for deep time. *Palaeogeography, Palaeoclimatology, Palaeoecology* 443: 98-106. https://doi.org/10.1016/j.palaeo.2015.11.041

Submitted on 15 February 2019;
accepted on 9 August 2019;
published on 14 May 2020.